This article is a *Plant Cell* Advance Online Publication. The date of its first appearance online is the official date of publication. The article has been edited and the authors have corrected proofs, but minor changes could be made before the final version is published. Posting this version online reduces the time to publication by several weeks.

Phototropin Influence on Eyespot Development and Regulation of Phototactic Behavior in *Chlamydomonas reinhardtii* [W]

Jessica Trippens,[a,1] Andre Greiner,[b,1] Jana Schellwat,[a] Martin Neukam,[a] Theresa Rottmann,[a] Yinghong Lu,[b,2] Suneel Kateriya,[c] Peter Hegemann,[b] and Georg Kreimer[a,d,3]

[a] Department of Biology, Friedrich-Alexander-University, 91058 Erlangen, Germany
[b] Institute for Experimental Biophysics, Humboldt University, 10115 Berlin, Germany
[c] Department of Biochemistry, University of Delhi South Campus, 110021 Delhi, India
[d] Erlangen Center of Plant Science, Friedrich-Alexander-University, 91058 Erlangen, Germany

The eyespot of *Chlamydomonas reinhardtii* is a light-sensitive organelle important for phototactic orientation of the alga. Here, we found that eyespot size is strain specific and downregulated in light. In a strain in which the blue light photoreceptor phototropin was deleted by homologous recombination, the light regulation of the eyespot size was affected. We restored this dysfunction in different phototropin complementation experiments. Complementation with the phototropin kinase fragment reduced the eyespot size, independent of light. Interestingly, overexpression of the N-terminal light, oxygen or voltage sensing domains (LOV1+LOV2) alone also affected eyespot size and phototaxis, suggesting that aside from activation of the kinase domain, they fulfill an independent signaling function in the cell. Moreover, phototropin is involved in adjusting the level of channelrhodopsin-1, the dominant primary receptor for phototaxis within the eyespot. Both the level of channelrhodopsin-1 at the onset of illumination and its steady state level during the light period are downregulated by phototropin, whereas the level of channelrhodopsin-2 is not significantly altered. Furthermore, a light intensity–dependent formation of a C-terminal truncated phototropin form was observed. We propose that phototropin is a light regulator of phototaxis that desensitizes the eyespot when blue light intensities increase.

INTRODUCTION

Motile algae have a virtually universal behavior that orients them toward places that best match the individual irradiation requirements for optimized photosynthesis without photodamage. The underlying predominant motility responses are either positive or negative phototaxis. This oriented movement, either toward or away from a light source, depends on light intensity and quality. To allow such precise movement responses, many flagellate algae of all major phylogenetic lineages have developed specialized optical devices (eyespots), which are antennae that determine the direction of incident light (Foster and Smyth, 1980; Kreimer, 1994).

In green algae, the eyespot is often peripherally located near the cell's equator and readily observable by bright-field microscopy as an orange- to red-colored spot. The ultrastructure of the functional eyespot involves local specializations of membranes from different compartments and highly ordered carotenoid-rich globules inside the chloroplast (Kreimer, 2009). The eyespot of *Chlamydomonas reinhardtii* is typically composed of two highly ordered layers of such globules, each subtended by a thylakoid membrane. The outermost globule layer is attached to specialized areas of both the chloroplast envelope and the adjacent plasma membrane. The globule layers modulate the light intensity reaching the photoreceptors in the plasma membrane patch as the cell rotates around its longitudinal axis during forward swimming. They function as a combined absorption screen and quarter-wave interference reflector. Thereby, the contrast at the photoreceptors is increased up to eightfold, making the whole optical system highly directional (Foster and Smyth, 1980; Kreimer and Melkonian, 1990; Harz et al., 1992; Kreimer et al., 1992). For phototaxis, *C. reinhardtii* uses the two unique photoreceptors, channelrhodopsin-1 (ChR1) and ChR2, which both act as direct light-gated ion channels. However, the extent to which phototaxis is supported by the different ChRs remains unclear (Nagel et al., 2002, 2003; Sineshchekov et al., 2002, 2009; Govorunova et al., 2004; Hegemann and Berthold, 2009).

In *C. reinhardtii*, the functional eyespot is assembled de novo after each cell division. This happens at a defined position within the cell and relative to the plane of the flagella (Holmes and Dutcher, 1989). The molecular mechanisms of its assembly and the dynamics of the eyespot are not understood in detail. Recent genetic and fluorescence microscope approaches identified some of the complexity of these processes. After cell division, ChR1 accumulates in the plasma membrane at the end of the

[1] These authors contributed equally to this work.
[2] Current address: Max-Planck-Institut für Molekulare Pflanzenphysiologie, 14476 Potsdam-Golm, Germany.
[3] Address correspondence to gkreimer@biologie.uni-erlangen.de.
The authors responsible for distribution of materials integral to the findings presented in this article in accordance with the policy described in the Instructions for Authors (www.plantcell.org) are: Peter Hegemann (hegemape@rz.hu-berlin.de) and Georg Kreimer (gkreimer@biologie.uni-erlangen.de).
[W] Online version contains Web-only data.
www.plantcell.org/cgi/doi/10.1105/tpc.112.103523

long 2s microtubular root, one of the four microtubular roots that are situated beneath the plasma membrane and extend from the basal bodies toward the posterior end of the cell, probably by directed vesicle transport. Acetylation of this microtubular root is an important clue for this process (Mittelmeier et al., 2011). In parallel, EYE2 (Cre12.g509250.t1.1), a protein required for assembly of eyespot globules, appears in the chloroplast envelope (Roberts et al., 2001; Boyd et al., 2011d). EYE3, a member of the ABC1 kinase family, is required for the formation of the globule layers and is localized to them (Boyd et al., 2011d). Furthermore, mutation in *MIN1* (Cre12.g490700.t1.1), which codes for a C2/LysM domain protein of unknown function, leads to miniature eyespots. MIN1 has been shown to be involved in chloroplast envelope interaction with the plasma membrane in the eyespot region (Mittelmeier et al., 2008). Proteomic analyses of purified eyespot fractions have shown the presence of many proteins thought to have structural functions and involvement in carotenoid sequestration. Proteins that are potentially important for signaling processes (e.g., protein kinases and photoreceptors), some of which are phosphorylated, have also been identified in the eyespot proteome (Schmidt et al., 2006; Wagner et al., 2008; Kreimer, 2009). Among the identified photoreceptors are four retinal-based photoreceptors (chlamyrhodopsin-1 and 2 as well as ChR1 and ChR2) and the flavin-based blue light receptor phototropin (Phot).

Phots are ubiquitous to vascular plants, ferns, mosses, and algae, and they function as light-activated receptor kinases (Briggs et al., 2001; Christie, 2007). *Arabidopsis thaliana* has two Phots, whereas the green algae *C. reinhardtii* and *Volvox carteri* have a single gene (Briggs et al., 2001; Huang et al., 2002; Prochnik et al., 2010). Phots possess two major functional regions: a photosensory region that contains two structurally similar light, oxygen, and voltage (LOV) domains (LOV1 and LOV2) that are located at the N terminus and a C-terminal Ser/Thr kinase, which belongs to the AGC-type kinase superfamily (Huala et al., 1997; Christie, 2007). Each LOV domain has a chromophoric group that is a flavin mononucleotide. Blue light induces covalent adduct formation between the flavin mononucleotide and a Cys residue of each LOV domain. This adduct formation induces conformational changes in both the LOV domains and the conserved amphipathic α-helix that is located downstream of LOV2. These structural changes lead to subsequent activation of the kinase, which is inhibited in the dark by association with LOV2 (Christie et al., 1999; Crosson and Moffat, 2002; Fedorov et al., 2003; Harper et al., 2003; Tokutomi et al., 2008).

LOV2 is essential for photosensing and LOV1 is thought to be important for attenuation of the light signal and for dimerization of Phot. Autophosphorylation is another prerequisite for initialization of signal transduction and is induced upon activation of the LOV domains (Christie et al., 2002; Salomon et al., 2003; Kinoshita et al., 2003; Matsuoka and Tokutomi, 2005; Kong et al., 2007; Inoue et al., 2008; Nakasako et al., 2008; Sullivan et al., 2008). The level of in vitro autophosphorylation differs between Phots of vascular plants and that of *C. reinhardtii* (Onodera et al., 2005). Also, the N terminus and the hinge region between LOV1 and LOV2 are shorter in Cr-Phot than those in the two At-Phots. Cr-Phot can functionally substitute Phot of vascular plants in vivo; therefore, the basic mechanisms of Phot action must be highly conserved, although physiological functions between vascular plant Phot and Cr-Phot are quite different (Huang et al., 2002; Onodera et al., 2005; Christie, 2007).

In vascular plants, Phot optimizes photosynthetic performance and fosters plant growth under weak light conditions. These functions include regulation of phototropism and stomata opening, chloroplast relocation movement responses, and leaf and cotyledon expansion and positioning (Liscum and Briggs, 1995; Kinoshita et al., 2001; Sakai et al., 2001; Kagawa and Wada, 2002; Sakamoto and Briggs, 2002; Ohgishi et al., 2004; Takemiya et al., 2005; de Carbonnel et al., 2010). Although Phot1 in *Arabidopsis* only has minor functions in transcriptional regulation, it destabilizes specific nuclear and chloroplast transcripts in response to high-intensity blue light (Folta and Kaufman, 2003; Ohgishi et al., 2004). This function is different in *C. reinhardtii*, for which Phot has been shown to cause major changes in expression of specific gene targets, particularly for genes encoding enzymes involved in chlorophyll and carotenoid biosynthesis (Im et al., 2006). Phot is also involved in both the regulation of multiple blue light–regulated steps during the reproductive life cycle and the chemotactic behavior of gametes from this alga (Huang and Beck, 2003; Ermilova et al., 2004; Huang et al., 2004).

To allow such diverse signaling processes upon activation, Phot must have divergent pathways and specific interaction partner(s). Several interacting proteins were recently identified in vascular plants (Kinoshita et al., 2003; Kaiserli et al., 2009; Sullivan et al., 2009; de Carbonnel et al., 2010; Tseng and Briggs, 2010). In *C. reinhardtii*, interacting proteins and the elements involved in downstream signaling are not known. Most of Cr-Phot is localized to the plasma membrane (Huang et al., 2002), so the situation in *C. reinhardtii* resembles that in vascular plants (Sakamoto and Briggs, 2002). A small proportion of Cr-Phot is also found in the flagella (Huang et al., 2004). Proteomic approaches confirm axonemal association and show the presence of Phot in the eyespot (Pazour et al., 2005; Schmidt et al., 2006). Until now, information about possible functions of Phot for either eyespot-related signaling or eyespot development was not available. Also, no detailed characterization of the effects of light on eyespot size in green algae is published. Therefore, the goals of this study were to (1) test possible light regulation of the eyespot size and (2) analyze the involvement of Phot in these processes. For the functional analyses, we used a Phot null mutant strain, mutant rescue, and overexpression approaches. Our results demonstrate that the eyespot size is dynamically regulated by light and Phot affects the algal primordial visual system and phototactic orientation in multiple ways.

RESULTS

Initial Evidence for Light Regulation of the Eyespot Size Was Obtained from *Tetraselmis astigmatica*

We obtained our first indications of light regulation of the eyespot size during a screening process for heterotrophically growing unicellular algae. Cells of the prasinophyte *T. astigmatica* possessed a significantly increased eyespot after growth in darkness

in the presence of Glc and yeast extract (Figures 1A and 1B). Compared with cells grown under a light/dark cycle in the same medium, the *T. astigmatica* eyespot size increased from 0.90 ± 0.26 μm^2 to 2.90 ± 0.80 μm^2. Maximal size was reached independent of cell division after 4 to 6 d of growth in darkness (Figure 1C). Furthermore, eyespot size was strongly dependent on light intensity during growth. When light intensity dropped below ~5 μmol m^{-2} s^{-1}, massive changes in eyespot size became evident (Figure 1D). Closer analysis of its spectral dependence only revealed wavelengths in the blue-green range as effective (Figure 1E). However, this alga was not sequenced, nor were standard molecular biological techniques established, hampering the molecular analyses of this process. Thus, the model green alga *C. reinhardtii* was used for the further analyses.

Eyespot Size of *C. reinhardtii* Is Dynamic and Regulated by Blue Light

The eyespot size in *C. reinhardtii* was analyzed under different growth regimes. We previously and briefly noted an eyespot size difference between *C. reinhardtii* laboratory strains (Kreimer, 2001, 2009); therefore, we conducted more detailed comparisons of eyespot sizes among eight different strains grown under standard light/dark cycles (14/10 h). A clear strain dependency of the eyespot size was observed, varying between 1.50 ± 0.42 μm^2 and 0.59 ± 0.17 μm^2 (Table 1). Among the strains we studied, the smallest eyespot was observed in the 302cw strain, which is also known to possess small cells. The other strains did not significantly differ in cell size, and no clear correlation between eyespot size and cell length was observed.

To investigate the dynamics of the eyespot, we analyzed the strain SAG73.72 in more detail. Culture age had no effect at 4 d (1.06 ± 0.28 μm^2, n = 126) or 21 d (1.05 ± 0.33 μm^2, n = 169), but eyespots were larger in cells grown in media with acetate as the carbon source (modified Gorman-Levine Tris-acetate-phosphate [TAP]) when compared with cells grown without additional carbon sources (MM; Table 1). Therefore, we conducted all further studies in the presence of acetate. Moreover, conversion of cells from the vegetative state into the sexually active, gametic state caused an eyespot size increase of ~35% (Table 1).

Eyespot size was also light dependent but less pronounced than that in *T. astigmatica* (Figure 2). The eyespot size of cells grown in darkness increased by ~50% compared with the eyespots of cells grown under moderate light intensities. By contrast, bright light induced a size reduction of ~30% compared with cells grown at 40 μmol m^{-2} s^{-1} (Figure 2A), and in all cases, blue light was more effective than other light colors (Figure 2B). These results led us to ask whether cells also adapt their eyespot size in response to duration of daily illumination and whether short light periods are sufficient to induce the response. We therefore grew cultures for 6 d under different light regimes that ranged from 1 to 24 h of blue light of the same intensity per day, and we measured eyespot sizes at the beginning of the light phase (Figure 2C). A progressive size reduction, in comparison to dark-grown cells, was seen for light periods beyond 1 h until ~50% was reached under continuous illumination. In summary, these data suggest that the eyespot size is dynamically regulated by a photoreceptor that absorbs in the blue region, and the duration of the daily illumination period is sensed by the cell. Several photoreceptors absorbing in this spectral region are known in *C. reinhardtii*, including ChR1, ChR2, a plant- and animal-like cryptochrome, and Phot (Huang et al., 2002; Nagel et al., 2003; Reisdorph and Small, 2004; Mittag et al., 2005).

Phototropin Is Involved in Eyespot Size Regulation

To obtain more information about the photoreceptors involved in the regulation of eyespot size, ChR1 knockout strains (ZF37-H2 and ZF37-H4) and a Phot knockout strain (ΔPhot^{G5}) that corresponds to G5 from Zorin et al. (2009) were analyzed. The absence of ChR1 and Phot proteins in the used strains was again confirmed with protein blots (see Supplemental Figure 1 online). For the ΔChR1 strains, we found no significant differences in eyespot size compared with the parental 302cw strain (ZF37-H2, 0.53 ± 0.12 μm^2, n = 83; ZF37-H4, 0.52 ± 0.11 μm^2, n = 96; 302cw, 0.52 ± 0.12 μm^2, n = 89). By contrast, eyespots of cells from ΔPhot^{G5} were significantly larger than those of the parental 302cw strain (Figures 3A and 3B). Furthermore, when light-grown cultures were transferred to darkness for 5 d, the eyespot size of ΔPhot^{G5} remained unchanged, whereas the eyespot size of 302cw cells increased to a level similar to that of the ΔPhot^{G5} strain. Upon transfer to the 14/10-h light/dark cycle, only the eyespots of the parental strain decreased in size (Figure 3C). Because the ΔPhot^{G5} strain was negative for phototropin in protein blots and the insertions were verified by PCR and DNA gel blotting (Zorin et al., 2009; see Supplemental Figure 1 online), these findings support the major involvement of Phot in the light regulation of eyespot size.

Next, we asked if overexpression of CrPhot could reconstitute eyespot size regulation in ΔPhot^{G5} cells and sought to identify the domain of CrPhot needed to induce decreased eyespot size. For all of our overexpression experiments to follow, we call the full-length phototropin "strain name_Phot," the LOV1+LOV2 domain "strain name_L1+L2," and the kinase part "strain name_Kin." Mutational inactivation of expressed domains is marked as either "~~L1+L2~~" or "~~Kin~~." Constructs C-terminally fused to the Zeocin resistance marker *sh*-Ble and their characteristics are summarized in Figure 3D and Supplemental Table 1 online.

The Kinase Domain of Phototropin Causes Light-Independent Reduction of Eyespot Size

Both the photochemical reaction in the LOV2 domain and the kinase activity are needed for light-dependent physiological responses in *Arabidopsis* (Briggs et al., 2001; Christie et al., 2002; Kong et al., 2006). By contrast, the kinase fragment alone can trigger light-independent responses (Kong et al., 2007). The ΔPhot^{G5} strain was transformed with plasmids, encoding full-length CrPhot that was C-terminally fused to the Zeocin resistance marker, *sh*-Ble, which should have restored photoregulation of eyespot size. We probed the expression of the Ble:Phot fusion protein in the ΔPhot^{G5} background using protein immunoblotting with an anti-*sh*-Ble serum (Figure 3E). Several protein bands, which were missing in untransformed ΔPhot^{G5} cells, were detected with the anti-*sh*-Ble serum. The uppermost band (~94 kD) corresponded to the full-length Ble:Phot fusion

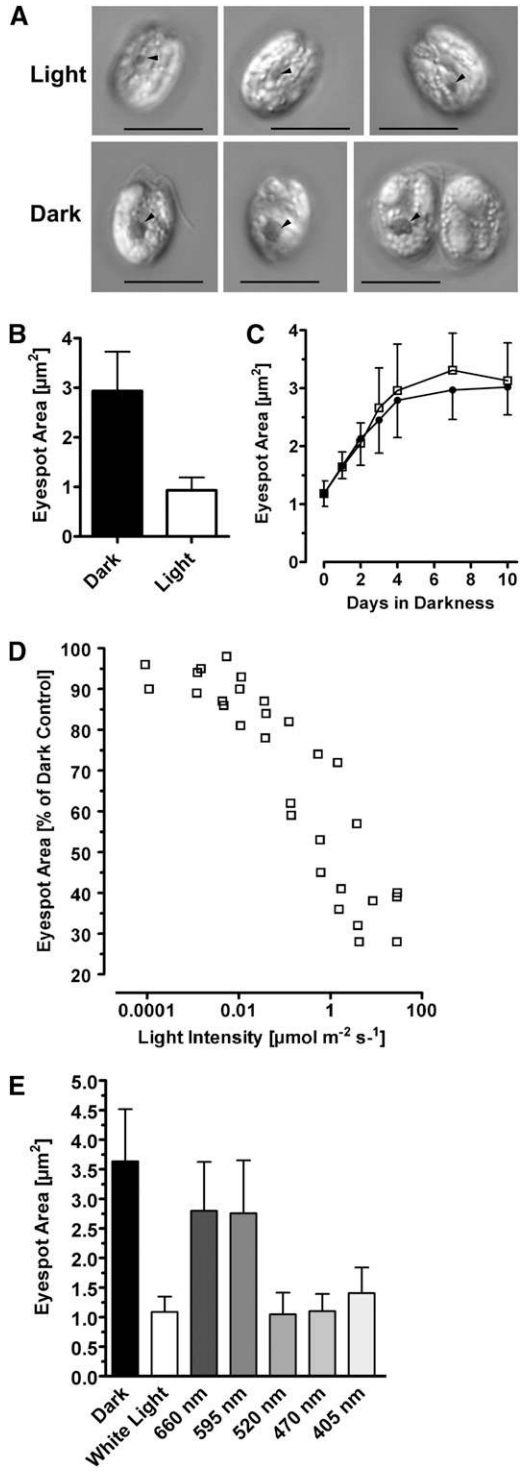

Figure 1. The Actual Eyespot Size of the Prasinophyte *T. astigmatica* Depends on Ambient Light Intensity during Growth.

(A) Differential interference contrast images of cells grown for 14 d in artificial seawater supplemented with Glc and yeast extract, either under a 14/10-h light/dark cycle (40 to 60 µmol photons m^{-2} s^{-1}) or in complete darkness. Arrowheads = eyespot. Bars = 10 µm.

protein, and the band at ~74 kD (PhotΔ20) corresponded to the proteolytic degradation product already identified by Pfeifer et al. (2010). This finding was unexpected because CrPhot degradation was not described in a previous study in which antibodies raised against the C-terminal kinase domain were used (Huang et al., 2004). We therefore characterized the formation of PhotΔ20 with the overexpression strains (Figures 3F and 3G). PhotΔ20 was also detected using an anti-LOV1 antiserum on different wild-type strains, thereby eliminating the possibility that its formation was an overexpression artifact. Moreover, PhotΔ20 formation was light induced and increased with light intensity. Furthermore, for ΔPhot^{G5} strains that expressed a light-insensitive, permanently inactive full-length Phot construct with mutated essential Cys residues of both LOV domains (Cys57Ser and Cys250Ser), no formation of PhotΔ20 was detectable (ΔPhot^{G5}_Phot_~~L1+L2~~, Figure 3F). This result suggests that thio-adduct formation and resulting conformational changes are needed for PhotΔ20 formation in *C. reinhardtii*. Identification of the truncated form by both antisera (anti-*sh*-Ble and anti-LOV1) suggests proteolytic cleavage at the C-terminal kinase domain. This mechanism produces, in vivo, an active Phot protein with inactive kinase in a light intensity–dependent manner.

Cells of the rescued ΔPhot^{G5}_Phot strain, grown under a normal light/dark cycle, had eyespots comparable to those of the parental strain, and upon transfer to darkness, eyespot sizes increased to values comparable to those in the ΔPhot^{G5} and parental strains (Figure 3H). We used ΔPhot^{G5}_Phot_~~L1+L2~~ as a control strain. This mutation completely abolished the light regulation of the eyespot size (Figure 3H). Next, we expressed the kinase without the LOV domains. ΔPhot^{G5}_Kin strains possessed smaller eyespots independent of the light regime. Their sizes were reduced to those observed in light for both the ΔPhot^{G5}_Phot strain and the parental strain (Figures 3H and 4A). The kinase domain sufficiently triggered light-independent eyespot

(B) Quantification of the eyespot area of dark- and light-grown *T. astigmatica* cells. Growth conditions same as in **(A)**. Mean ± SD; $n = 37$ cells. Difference is highly significant (Student's t test, $P < 0.0001$).

(C) Eyespot size increases in darkness, independent from cell growth. Cells were grown in either plain artificial seawater (filled circles) or artificial seawater supplemented with Glc and yeast extract (open squares), which allowed population growth. Cell densities were 2.2 to 2.5 × 10^5 cells mL^{-1} at the start and 2.9 × 10^5 cells mL^{-1} (no additions) and 1.7 × 10^6 cells mL^{-1} (Glc + yeast extract) at the end. Mean ± SD; $n = 35$ to 37 cells. Values obtained for the eyespot sizes were not significantly different (Student's t test, $P = 0.4003$).

(D) Cultures were grown for 22 d at the indicated light intensities of white light in a 14/10-h light/dark cycle. Each data point represents the mean eyespot area of 35 to 90 cells. For clarity, SD is not shown. Light intensities > 0.015 µmol photons m^{-2} s^{-1} represent measured values; values below that were calculated using the measured values, at 537 nm, of LOT neutral density filters.

(E) Spectral dependence of the eyespot size reduction. Cells were grown at the indicated wavelengths as described in **(D)**. Light intensities varied between 12 and 80 µmol photons m^{-2} s^{-1}. For each wavelength, 53 to 87 cells were analyzed. Mean ± SD; differences are significant (one-way ANOVA, $P < 0.0001$).

Table 1. Eyespot Area in *C. reinhardtii* Depends on Strain, Growth Medium, and Life Cycle Stage[a]

Strain	Eyespot Area ± SD (μm^2)	*n*	Growth Medium
CC124 mt^-	1.31 ± 0.36	227	TAP
CC125 mt^+	1.20 ± 0.39	111	TAP + Arg
SAG 73.72 mt^+ (vegetative)	1.07 ± 0.26[b,c,d]	170	TAP
SAG 73.72 mt^+ (vegetative)	0.85 ± 0.28[b,d]	153	MM
SAG 73.72 mt^+ (gametic stage)	1.45 ± 0.30[c,d]	113	NMM[e]
CC-4051	0.95 ± 0.24	166	TAP
302cw	0.59 ± 0.17	254	TAP + Arg
MS-325	1.00 ± 0.24	105	TAPTY
CC 621 mt^-	1.50 ± 0.42	185	TAP
CC 620 mt^+	1.29 ± 0.45	198	TAP

[a]All strains were grown under identical conditions for 4 to 6 d, at 40 to 60 μmol photons m^{-2} s^{-1} white light, and a 14/10-h light/dark cycle.
[b,c]Significantly different means (Student's *t* test, $P < 0.0001$).
[d]Significantly different means (ANOVA, $P < 0.0001$).
[e]Cells were first grown for 5 d in TAP, followed by transfer to NMM for 2 d.

size reduction. To further confirm this conclusion, Asp-547 and Ser-611 were separately mutated, yielding ΔPhot^{G5}_~~Kin~~ #1 and ΔPhot^{G5}_~~Kin~~ #2 strains. These positions correspond to Asp-806, which is responsible for Mg^{2+}-ATP coordination, and Ser-851, which is needed for autophosphorylation in At-Phot (Christie et al., 2002; Inoue et al., 2008). Both mutations completely suppressed the eyespot size reduction that we observed in the ΔPhot^{G5}_Kin strains (Figure 4A). The eyespots in both ΔPhot^{G5}_~~Kin~~ strains had sizes in the range observed in the ΔPhot^{G5} or ΔPhot^{G5}_Phot_~~L1+L2~~ cells, which expressed full-length Phot with abolished photoreactivity (Figures 3H and 4). To rule out the possibility that the observed differences in eyespot size were correlated to differences in cell size, cell length and eyespot area of ΔPhot^{G5}, ΔPhot^{G5}_Phot, and ΔPhot^{G5}_Kin cells were measured in parallel. No correlation between eyespot area and cell length was observed (see Supplemental Figure 2 online).

Photosensory LOV Domains Alone Can Also Trigger Eyespot Size Reduction

The two Phot LOV domains exhibit different functions: LOV1 is thought to be important for dimerization and act as an attenuator of Phot activity, whereas LOV2 has a central role in photoreceptor light activation and regulation of the kinase activity (Demarsy and Fankhauser, 2009). Since we detected a light-induced formation of a C-terminal truncated Phot fragment (PhotΔ20; Figures 3E to 3G), we examined the influence of the LOV1+LOV2 fragment on eyespot size regulation. Interestingly, we also observed eyespot size reduction in ΔPhot^{G5}_L1+L2 strains (Figure 4B). This effect was reverted by either point mutation of both essential Cys residues in LOV1+LOV2 (ΔPhot^{G5}_~~L1+L2~~) or mutation of Cys-250 in LOV2 (ΔPhot^{G5}_L1+~~L2~~). By contrast, inactivation of the LOV1 domain by mutation of Cys-57 resulted in an intermediate, yet significant, eyespot size reduction (ΔPhot^{G5}_~~L1~~+L2; Figure 4B). These results show that the N-terminal photoreceptor domain itself can at least partially initiate a signaling process that leads to light-dependent eyespot size regulation.

Expression of Phototropin Constructs in Phototropin Wild-Type Backgrounds Affects Eyespot Size

To exclude possible strain-specific effects, Phot constructs were also overexpressed in strains that possess Phot and functional flagella. Unfortunately, both 302cw and ΔPhot^{G5} do not possess flagella. As exemplified in Figure 3G, which shows the full-length Ble:Phot construct in a wild-type background, the level of expression did not exceed that of endogenous crPhot. Strains MS325, which is a backcross of 302cw into a flagellated strain, and CC125 were both analyzed in detail. MS325 cells have an intermediate-sized eyespot, and CC125 has a slightly larger one (Table 1). Expression of ~~L1~~+L2 in the MS325 background induced a reduction of the eyespot area by ~30% in comparison to the wild type grown under identical conditions. However, overexpression of Phot with inactivated LOV domains had no effect (see Supplemental Figure 3 online).

The influence of kinase domain overexpression was analyzed in a CC125 background. Here, aggregates of either two or more cells were induced within the mother cell wall (palmelloids) in a manner that was independent of the time point in the light phase (see Supplemental Figure 4 online). This phenotype is indicative of effects on hatching, a process that involves Phot (Huang and Beck, 2003). In addition, transcriptional down-regulation of an outer cell wall glycoprotein (GP2) was observed in a CrPhot knockdown strain (Im et al., 2006). Palmelloids were not observed in the ΔPhot^{G5}_Kin strains due to the lack of a cell wall in the cw background. CC125_Kin cells were therefore liberated from the mother cell walls by autolysin treatment prior to measurement. The eyespot size was reduced by ~30% in these transformants (CC125, 1.20 ± 0.39 μm^2, $n = 111$; CC125_Kin, 0.84 ± 0.21 μm^2, $n = 122$; Student's *t* test, $P < 0.0001$).

Phototropin Affects ChR Levels

Because Phot is involved in eyespot size regulation, we were also interested in its potential regulation of ChRs. Therefore, crude extracts of ΔPhot^{G5} and 302cw cells grown under different light intensities were analyzed for their ChR1 levels with protein gel blot analyses (Figure 5A). To avoid possible light-induced

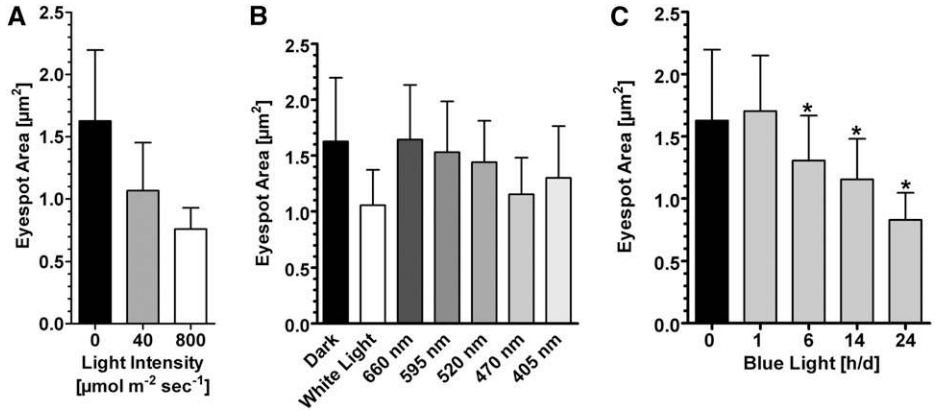

Figure 2. Light Regulation of Eyespot Size in *C. reinhardtii*.

(A) Quantification of the eyespot area of cells from strain SAG73.72 mt+, grown in either complete darkness or at the indicated light intensities of a 14/10-h light/dark cycle (mean ± SD; n = 234 cells [dark], and n = 243 cells [40 µmol m^{-2} s^{-1}] and 313 cells [800 µmol photons m^{-2} s^{-1}]], for 5 to 6 d. Differences are significant (one-way ANOVA, $P < 0.0001$).

(B) Quantification of the eyespot area (mean ± SD) of SAG73.72 cells grown under a 14/10-h light/dark cycle for 5 to 6 d at the indicated wavelengths. Light intensities were as in Figure 1E. For each wavelength, 187 to 293 cells were analyzed. Only cells exposed to 405 nm, 470 nm, and white light showed a significant eyespot size reduction ($P < 0.0001$) when compared with dark-grown cells.

(C) Quantification of the eyespot size of SAG 73.72 cells grown for 6 d either under complete darkness or with the indicated blue light (470 nm)/dark cycle (80 µmol photons m^{-2} s^{-1}; mean ± SD; n = 144–255 cells; *one-way ANOVA, $P < 0.0001$).

changes in the ChR1 level, samples were taken at the end of the dark phase, just before the onset of the illumination period. When grown under low light intensity (25 µmol m^{-2} s^{-1}), the ChR1 starting levels were almost identical in both strains. Increasing light intensities resulted in a steep drop of the ChR1 starting amount in the 302cw strain. At 110 µmol m^{-2} s^{-1}, only ~15% of the level observed at 25 µmol m^{-2} s^{-1} was still detectable. No further decrease occurred at higher intensities. By contrast, in ΔPhot^{G5} cells, the ChR1 starting levels remained unchanged up to ~60 µmol m^{-2} s^{-1}. Upon growth at higher intensities, we also observed lower ChR1 levels in this strain (Figure 5A). The decrease in eyespot area of 302cw cells (~50%) did not correlate with the drop in the ChR1 level (~85%). These results, in conjunction with an unchanged eyespot size in the ΔChR1 strains, indicate that a simple correlation between eyespot area and ChR1 content likely does not exist. This assumption is corroborated by immunoblot analyses of crude extracts that were obtained from both strains during the middle of the illumination period. Here, the ChR1 level in the ΔPhot^{G5} cells was also always higher than that in the wild type (Figure 5B).

The higher ChR1 level in ΔPhot^{G5} cells cannot be attributed to effects on the cell cycle, as cell densities at the onset of illumination and at 17 h were identical. Therefore, CrPhot might affect eyespot size and ChR1 level differentially. To obtain further experimental evidence for this assumption, we also analyzed the ChR1 levels in ΔPhot^{G5}_Kin and ΔPhot^{G5} strains that were overexpressing LOV1+LOV2. No significant effects on the ChR1 levels were observed for either ΔPhot^{G5}_~~L1~~+L2 or ΔPhot^{G5}_L1+~~L2~~ strains (see Supplemental Figure 5 online), but overexpression of the kinase domain had a strong effect. Compared with 302cw cells, the ChR1 level in ΔPhot^{G5}_Kin was already downregulated in the dark (Figure 5C). Light induced a further reduction of the ChR1 level, suggesting the existence of an additional light-dependent regulatory mechanism of the ChR1 level. Also, kinase domain overexpression in the Phot-containing CC125 background affected the ChR1 level, decreasing it by ~75% (Figure 5D). Under identical growth conditions, the eyespot area of the CC125_Kin strain was only reduced by ~30%. The discrepancy between the reductions in the ChR1 level and eyespot size was slightly more pronounced in ΔPhot^{G5}_Kin cells, in which ChR1 levels were reduced by ~80% and eyespot area decreased by only 18% (302cw, 0.56 ± 0.11 µm², n = 147, ΔPhot^{G5}_Kin, 0.46 ± 0.13 µm², n = 142).

Besides the effects on ChR1 stability, the above discrepancy might be due to limitations in detecting very small eyespots with differential interference contrast microscopy. In many ΔPhot^{G5}_Kin cells, the eyespot was not clearly identifiable and could not be included in size determinations. Indirect immunofluorescence microscopy, using the anti-ChR1 serum, was used to exclude the possibility that only a subpopulation of the ΔPhot^{G5}_Kin cells possessed an eyespot (Figure 5E). Cells were also stained for acetylated tubulin to visualize, in parallel, the relative position of the eyespot in relation to acetylated microtubular rootlets. In *C. reinhardtii*, the eyespot is always associated with the 2s microtubular root of the four roots that emerge from the basal bodies (Holmes and Dutcher, 1989). Acetylation of this root typically extends longer into the cell and may be related to asymmetric localization of the ChR1 patch (Boyd et al., 2011a; Mittelmeier et al., 2011). The typical position of the ChR1 patch was not disturbed in the kinase overexpression strain, and patches, although somewhat smaller, were observed in the vast majority of these cells (Figure 5E).

We were also interested in determining whether ChR2 levels were affected by Phot, similar to above. Interestingly, the ChR2 level in ΔPhot^{G5}_Kin cells did not decrease (Figure 5F). Compared with the wild type, the level was even slightly increased.

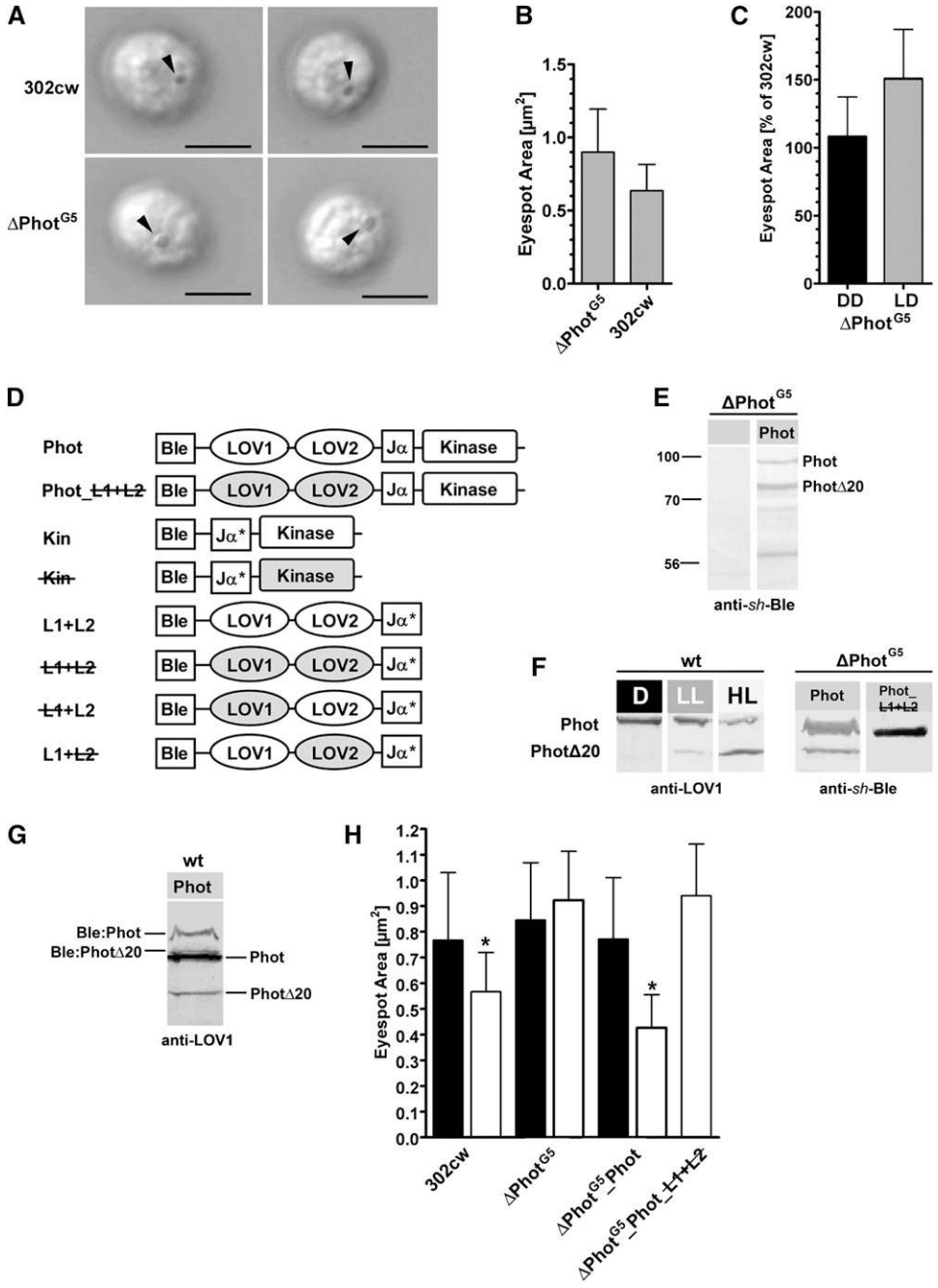

Figure 3. Light Regulation of Eyespot Size Is Not Detected in the Phototropin-Deficient Strain ΔPhot^{G5} and Can Be Restored by Overexpression of Phototropin.

(A) Differential interference contrast images of cells from both the ΔPhot^{G5} and its parental strain (302cw) grown under the standard 14/10-h light/dark cycle (white light; 40 to 60 μmol photons m^{-2} s^{-1}). Arrowheads = eyespots. Bars = 5 μm.

(B) Quantification of the eyespot area of the ΔPhot^{G5} strain (mean ± SD; n = 101) and strain 302cw (n = 165) grown under the standard light/dark cycle. The difference is highly significant (Student's t test, $P < 0.0001$).

(C) Eyespot area of ΔPhot^{G5}, in relation to that of the parental strain, under different light conditions during growth. Cells from both strains were grown for 5 d in darkness (DD) and then transferred to the normal 14/10-h light/dark cycle (LD). Eyespot areas were determined at the end of the growth phase in complete darkness and at the beginning of day 5 under the normal light regime (mean ± SD; n = 109 to 181 cells; one-way ANOVA, $P < 0.0001$).

(D) Designations and schematic drawings of the organization of the Ble:Phot constructs used for transformation of ΔPhot^{G5} and other *C. reinhardtii* strains. Inactivated domains are highlighted in gray. Jα* = partially present Jα domain.

This observation raised the possibility that a decrease in ChR1 might be counterbalanced by the cells through an increase in ChR2. Such a massive increase in ChR2 was reported for a *C. reinhardtii* RNA interference strain (Govorunova et al., 2004). By such a mechanism, the eyespot size might remain at a level identical to that in the ΔChR1 strains. To test this hypothesis, protein gel blot analyses, using an anti-ChR2 serum, were conducted on ΔChR1 strains in the 302cw background. Only minor changes in the ChR2 level were evident in both ΔChR1 strains in the three independent experiments (Figure 5G). Quantification of the dark levels yielded 108.0% ± 8.4% for strain ZF37-H2 and 105.7 ± 12.7% for strain ZF37-H4, relative to strain 302cw. Therefore, eyespot size and ChR2 levels do not appear to be interrelated with ChR1 levels in these ΔChR1 strains. This result further confirms the finding that ChR2 promoter activity is only reduced under high light conditions (Fuhrmann et al., 2004).

The above results show that ChR1 and not ChR2 is a target for Phot regulation. In summary, Phot might affect the ChR1 level in at least two different ways: (1) by affecting the actual eyespot size and (2) by influencing either ChR1 stability or degradation at later time points during the light phase.

Phototactic Behavior and Adaptive Responses Are Affected by Phototropin

We also analyzed phototactic behavior of cells that overexpressed CrPhot constructs in flagellated backgrounds. To achieve a uniform response in the population, gametes were used in these experiments. Gametes of the wild-type strain CC125 showed normal photoresponses (i.e., 470-nm blue light induced a positive phototactic movement, whereas a near-UV light of 405 nm caused an avoidance response; Figure 6A). Dark- and light-adapted CC125 gametes showed qualitatively similar behavior, except in dark-adapted cells, in which phototactic rate and light sensitivity were reduced. Overexpression of the kinase domain switched the sign of phototaxis from positive to negative upon blue light illumination, whereas UV light induced a slightly stunted response peak. Interestingly, the difference seen in CC125, between light- and dark-adapted cells, was completely abolished in CC125_Kin (Figure 6A).

We were surprised that overexpression of the LOV domains also affected eyespot size (Figure 4B), and this prompted our interest in the phototactic behavior of these strains. Although functional LOV domains fused to the Ble-marker were readily overexpressed in the ΔPhot^{G5} strain, our attempts to express these constructs in CC125 were not successful. As such, we used the cell wall–deficient strain, CC3403, which can be transformed with higher efficiency. Figure 6B shows the behavior of light-adapted cells from strain CC3403 as a reference and that of the strain overexpressing the functional LOV1+LOV2 construct (CC3403_L1+L2). In the parental strain, the first application of blue light triggered a negative phototactic response, which differed from the response by strain CC125. Changes in phototactic behavior during the first seconds of illumination often occur and are well documented for different *C. reinhardtii* strains (Hegemann and Berthold, 2009). After this initial response, the behavior was similar to that in CC125. As observed for the CC125_Kin cells, the CC3403_L1+L2 cells showed inverted phototactic behavior upon 470-nm and UV illumination when compared with cells of the parental strain. Interestingly, dark-adapted CC3403_L1-L2 cells had delayed responses to the first blue light illumination, but later had no delays. This suggests that LOV1+LOV2 interactions with the endogenous Phot kinase domain and/or other targets might be involved in phototactic behavior. To test this hypothesis, we also expressed a double-blind version of the LOV1+LOV2 construct (~~L1+L2~~), which inhibited photoactivation and mimicked the dark state of CrPhot (Figure 6C). Light-adapted CC3403_~~L1+L2~~ cells showed responses similar to those in CC3403_L1+L2, and their responses were, again, inverse to those of CC3403. By contrast, dark-adapted CC3403_~~L1+L2~~ cells showed almost no phototaxis. Responses of dark-adapted CC3403 gametes were used as control (Figure 6C). Under these conditions, previous activation of endogenous Phot and an interaction with the ~~L1+L2~~ domains can be excluded, which could have led to inactivation of the kinase domain in the endogenous Phot. This result suggests that LOV domains in the dark state interact with the target(s), leading to the suppression of phototaxis.

DISCUSSION

The green algal eyespot has long been regarded as a relatively static structure that is specialized for light perception and modulation. Only recently has the idea evolved that the algal eyespot is a dynamic structure that is partially interrelated with plastoglobules and is probably involved in other physiological processes (Kreimer, 2009; Boyd et al., 2011d). Here, we showed

Figure 3. (continued).

(E) Immunoblot analysis of crude cell extracts from ΔPhot^{G} and ΔPhot^{G5}_Phot strains, using anti-*sh*-Ble (1:2000). Phot, full-length Phot fusion protein; PhotΔ20, truncated Phot fusion protein, cleaved in the C-terminal kinase domain. Proteins were separated on a 10% SDS-PAGE gel.

(F) Formation of the PhotΔ20 variant is light dependent. Dark-adapted CC124 wild-type cells (wt) were exposed to either low light (LL = 0.5 μmol photons m^{-2} s^{-1}) or high light (HL = 90 μmol photons m^{-2} s^{-1}). Crude extracts were probed with anti-LOV1 serum (1:2000). As a negative control for light-induced degradation, the nonphotoactivable Ble:Phot fusion protein, Phot_~~L1+L2~~, was expressed in the null background (ΔPhot^{G5}_Phot~~L1+L2~~). ΔPhot^{G5} was used as a reference. Both strains were exposed to white light (40 μmol photons m^{-2} s^{-1}). D, dark.

(G) Levels of the Ble:Phot fusion protein, and its degradation product Ble:Phot Δ20, are lower than those of endogenous Phot in the cw15ArgA_Phot strain (wt_Phot). Cells were exposed to 40 μmol photons m^{-2} s^{-1} of white light, and the extract blot was probed with anti-LOV1 antiserum.

(H) Cells of 302cw, ΔPhot^{G5}, and transformants of the ΔPhot^{G5} background, expressing either a functional phototropin (ΔPhot^{G5}_Phot) or a phototropin with inactivated LOV domains (C57S and C250S; ΔPhot^{G5}_Phot_~~L1+L2~~), were grown for 4 d in either complete darkness (black bars) or the standard light/dark cycle (white bars) prior to eyespot area quantification (mean ± SD; *n* = 51 to 181 cells; *one-way ANOVA, $P < 0.0001$).

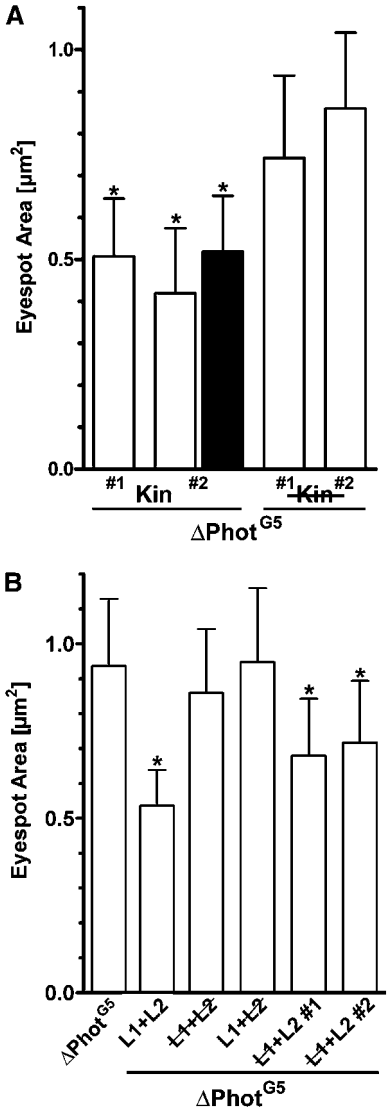

Figure 4. Both the Kinase Domain and the Photosensory Domain of Phototropin Are Involved in Eyespot Size Regulation.

(A) Eyespot areas of independent transformants expressing either the functional kinase domain (ΔPhot^{G5}_Kin #1 and #2) or an inactive kinase domain (point mutations either in the ATP binding site [ΔPhot^{G5}_~~Kin~~ #1; D547N] or in an essential autophosphorylation site [ΔPhot^{G5}_~~Kin~~ #2; S611A]). Cells were grown for 4 d either under the standard light/dark cycle (white bars) or in complete darkness (black bars) prior to measurements (mean ± SD; n = 50 to 119 cells; *one-way ANOVA, $P < 0.0001$).
(B) Eyespot areas of strains ΔPhot^{G5}, ΔPhot^{G5}_L1+L2 (expressing functional LOV domains), ΔPhot^{G5}_~~L1+L2~~ (expressing a construct with both LOV domains inactivated by point mutations C57S and C250S), ΔPhot^{G5}_L1+~~L2~~ (strain with an inactivated LOV2 domain), and ΔPhot^{G5}_~~L1~~+L2 #1 and #2 (independent strains with inactivated LOV1 domains). Cells were grown under the standard light/dark cycle (mean ± SD; n = 91 to 118; *one-way ANOVA, $P < 0.0001$).

that both eyespot size and the level of ChR1, the major primary photoreceptor for phototaxis in *C. reinhardtii*, are dynamically regulated by light. We also showed that the blue light photoreceptor Phot has a major and unique function in these regulatory processes. Effects of blue-green light were also observed in the eyespot of the marine prasinophyte, *T. astigmatica*, indicating that size adaptation of the eyespot to ambient light might be widespread among the Chlorophyta.

Motile green algae must precisely sense their light environment and be able to respond to changes on a short and an intermediate time scale. Here, both intensity and daily duration of illumination period affected eyespot size. Phot allows relatively low light intensities to evoke such responses for two reasons: (1) Blue light can penetrate deeply into the water column, and (2) the lifetime of the light-activated LOV domains in *C. reinhardtii* range from several seconds to minutes (Guo et al., 2005). Since Phot kinase activation also does not occur at very low light intensities (Christie et al., 2002), we believe Phot is an ideal photoreceptor for the regulation of eyespot size.

Phot has recently been identified in the eyespot proteome (Schmidt et al., 2006), but its function in phototaxis and eyespot development was hitherto unknown. Our observations of light-insensitive eyespot size in the ΔPhot^{G5} strain and its restoration by overexpression of full-length Phot or its kinase part clearly links functions of Phot to the eyespot and the photoresponses of *C. reinhardtii*. The specificity of the observed effects is supported by our observation that inactivation of either the LOV domains or the kinase domain prevents functional complementation. The different effects on ChR1 content (e.g., either its massive, light-independent decrease upon overexpression of the kinase domain or its prevented decrease in ΔPhot^{G5} cells in the light) directly link Phot to phototaxis. Similar to observations in vascular plants, where the kinase fragment alone modifies physiological responses in a light-independent manner (Kong et al., 2007), our data show that the active kinase domain of CrPhot is sufficient to cause a light-independent reduction of eyespot size and a decrease in ChR1 content and mimic a high-light situation in phototactic behavior. The kinase activity of Phot is therefore essential for long-term light adaptation of phototaxis.

Although the photosensory N terminus in *Arabidopsis* was not sufficient to evoke physiological responses in planta (Kong et al., 2007), we observed clear effects of the N-terminal photoreceptor fragment on eyespot size. These effects were seen in the absence as well as in the presence of endogenous Phot. As we will discuss in detail later, it also affected phototactic behavior. This activity of the LOV1+LOV2 domain, without the kinase, might be related to the formation of PhotΔ20 by cleavage of CrPhot within the kinase domain in the wild type. This mechanism produces an additional photoreceptor form that has an inactive kinase but still has active LOV domains in vivo. The ratio of both forms depended on light intensity: Under high-light conditions, the proportion of PhotΔ20 increased (Figure 3F). As such, we propose that the fully active Phot and the PhotΔ20 act synergistically in signaling in *C. reinhardtii* and that LOV1+LOV2 overexpression might artificially mimic a high-light situation.

Phototactic behavior, eyespot size, and ChR1 content are likely affected by several different signaling pathways. The importance of the fully active form of crPhot in these signaling cascades is

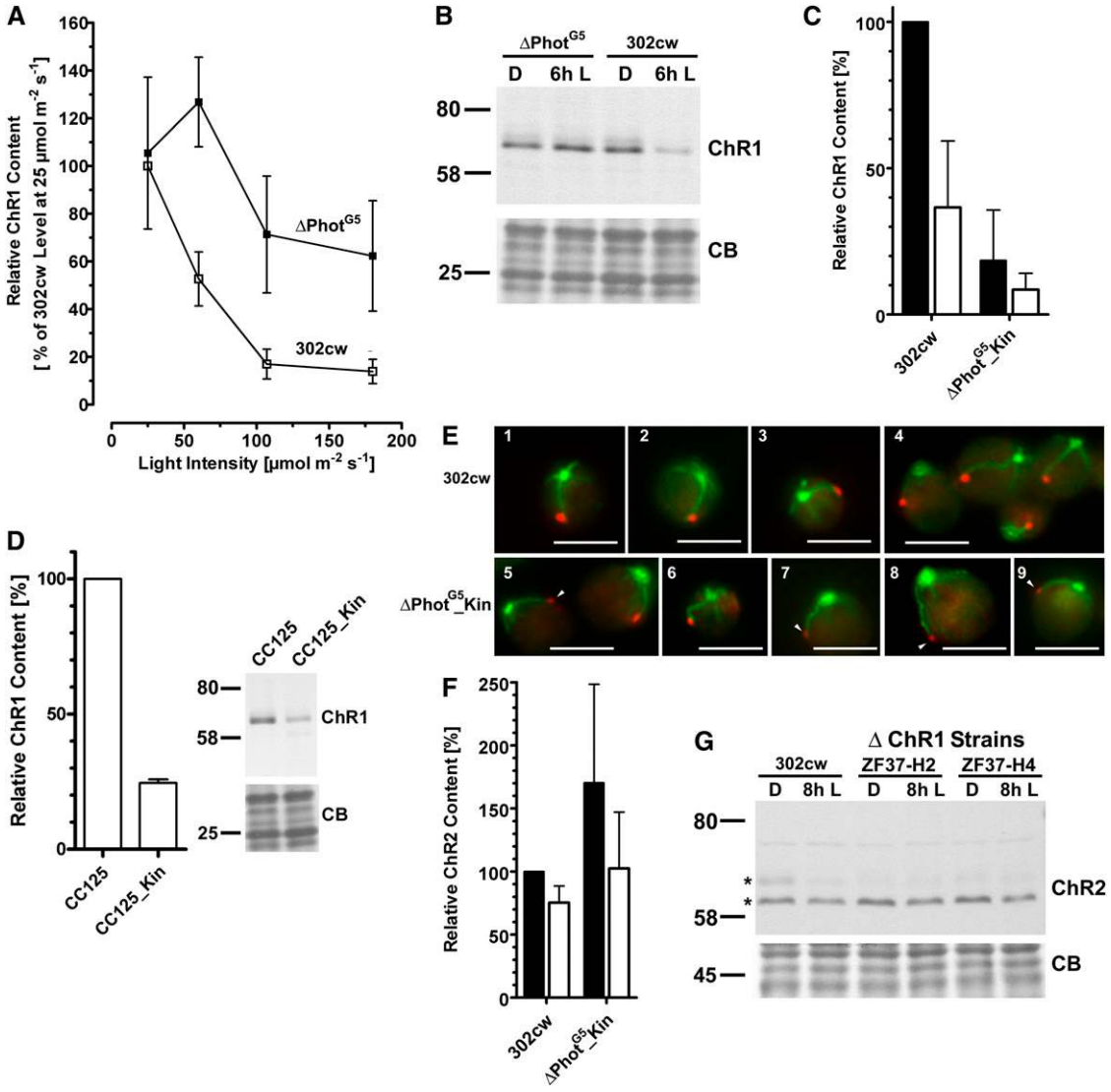

Figure 5. Phototropin Is Involved in the Regulation of ChR Content.

(A) Quantitative gel blot analyses of crude extracts of strains 302cw (open squares) and ΔPhot^{G5} (closed squares), which revealed that the ChR1 content, before onset of illumination, depends on ambient light intensity during growth, and Phot. Crude extracts of cells, grown at the indicated light intensities, were made directly before the onset of illumination under red safety illumination. Proteins (8 µg) were separated by SDS-PAGE (11%) and used for protein gel blot analysis with an anti-ChR1 antiserum (ChR1, 1:5000). Equal loading was verified by Coomassie blue staining. Data points represent mean ± SD of three independent biological replicates.

(B) ChR1 levels in the ΔPhot^{G5} strain are higher in the light than those in its parental strain. Crude extracts were made either directly before (D) or 6 h after the onset of illumination (6h L). Other procedures were the same as in **(A).** Coomassie blue (CB) is the loading control.

(C) Overexpression of the Phot-kinase domain results in a strong, light-independent ChR1 reduction. Crude extracts of the indicated strains were prepared from cells grown at 60 µmol m^{-2} s^{-1}, either directly before (black bars) or 8 h after onset of illumination (white bars). Experimental details were the same as described in **(A)**.

(D) Phot kinase domain overexpression in the CC125 background leads to significantly less ChR1. Crude extracts were prepared from cells 7 h after the onset of illumination. Experimental details were the same as in **(A)**.

(E) Positioning of the ChR1 spot adjacent to the long, acetylated 2s microtubular root is not affected in ΔPhot^{G5}_Kin. Cells of 302cw (1 to 4) and ΔPhot^{G5}_Kin (5 to 9). Merged fluorescence images of cells labeled with anti-ChR1 (red) and antiacetylated tubulin (green). Arrowheads = faint ChR1 fluorescence signals. Bars = 5 µm.

(F) ChR2 levels did not decrease in ΔPhot^{G5}_Kin. Gel blot analyses (7% SDS-PAGE) using an anti-ChR2 antiserum (1:1000) were performed with the same extracts as in **(C)**. Data represent mean ± SD of three quantifications (sum of both ChR2 bands; see asterisks in **[G]**).

(G) The ChR2 levels in two ΔChR1 strains were not significantly altered compared with the parental strain. Cells were grown as described in **(C)**, and extracts were made either directly before (D) or 8 h after the onset of illumination (8h L). Asterisks denote the two ChR2 bands.

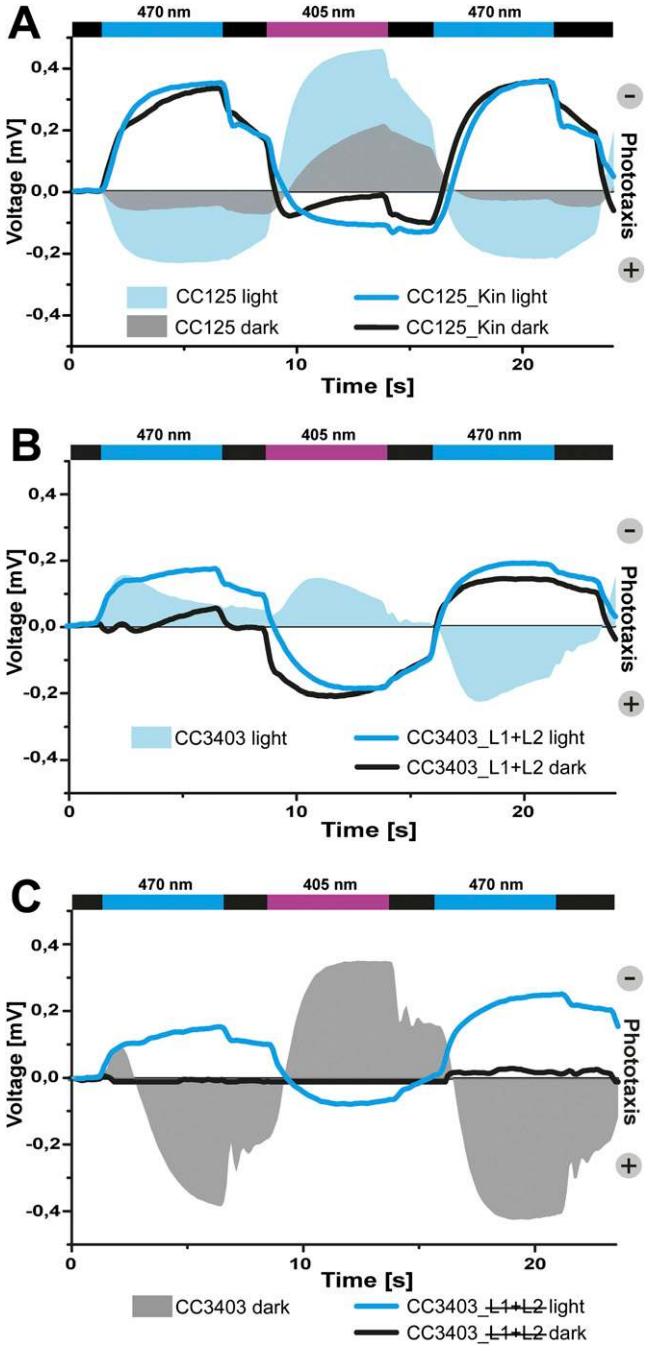

Figure 6. Phototropin-Dependent Changes in Phototactic Behavior of Gametes, as Determined by Light-Scattering Measurements.

(A) Wild-type strain CC125 exhibits normal phototactic responses. Blue light (470 nm) induces a positive phototactic movement, whereas strong, near-UV light (405 nm) induces an avoidance response. Dark-incubated cells of CC125 show the same amplitude phase shift as light-adapted cells, but the altitude is reduced. Overexpression of the C-terminal, CrPhot kinase domain in CC125 (CC125_Kin) causes negative phototaxis upon blue light illumination. Differences observed in the wild type between light- and dark-adapted cells are missing in the kinase overexpressing cells. Illumination with 405-nm light caused only a weak response. Light from light-emitting diodes of 470 and 405 nm was applied for 5 s, interrupted by a 2-s dark phase.

(B) L1+L2 overexpression in the CC3403 background (CC3403_L1+L2) causes an inversion of the phototactic response. Light-adapted CC3403 cells are shown as a reference. Differences between light- and dark-adapted cells are abolished after the first light phase.

(C) Overexpression of inactivated LOV domains (~~L1+L2~~) in dark-adapted cells causes inhibition of phototaxis. In light-adapted cells, no inhibition is observed. Responses of dark-adapted CC3403 cells are given as a reference.

supported by our observation that kinase domain overexpression affected all three processes. By contrast, the LOV1+LOV2 domain constructs failed to influence the ChR1 content, pointing to differences in the signaling routes between both Phot forms. We do not know whether Phot and PhotΔ20 act on identical or different target(s). Both species might even differ in target interaction strength or complex formation. As we will discuss later, the LOV domains of PhotΔ20 might additionally interact with proteins exhibiting structural similarities to the Phot kinase domain, allowing signal input via different proteins.

Currently, no direct interacting partner of Phot has been identified in *C. reinhardtii*, and the cellular targets resulting in a decreased eyespot size remain elusive. Different eyespot assembly and positioning mutants have been characterized during the last years, including miniature and eyeless mutants (Mittelmeier et al., 2008; Boyd et al., 2011a, 2011b, 2011c, 2011d). These proteins might be affected and may even be a part of the signaling cascade(s) that is initiated by Phot activation and leads to an eyespot size adapted to ambient light conditions. Additionally, targets of Phot signaling may not be directly involved in eyespot size regulation. Our compiled data pinpoint ChR1, but not ChR2, as one of these proteins. ChR1's cellular level is considerably higher than that of ChR2, although the extent to which phototaxis is supported by the two ChRs is still unclear (Hegemann and Berthold, 2009; Sineshchekov et al., 2009). Although the presence of ChRs might have an important impact during eyespot assembly (Boyd et al., 2011c), our data on the ΔChR1 strains showed that the size of the eyespot is not affected by a complete absence of ChR1. Furthermore, overexpression of the kinase domain caused a strong ChR1 decrease in both $\Delta Phot^{G5}$ and CC125 cells, whereas the eyespot size was only slightly affected. Phot proteins dimerize and are supposed to either cross- or autophosphorylate (Kaiserli et al., 2009). Overexpression of the kinase domain alone might cause hyperactivation of the endogenously expressed Phot and other Phot targets to an extent that probably simulates a high-light state. As a response, the ChR1 level might be decreased. This interpretation is corroborated by the observation that the ChR1 level in $\Delta Phot^{G5}$ cells remains high after 6 h of illumination. ChRs can be phosphorylated in vivo (Wagner et al., 2008), but we do not know whether they are directly phosphorylated by Phot or whether Phot affects their phosphorylation status more indirectly (e.g., by regulating phosphatases).

Phototactic behavior of the CC125_Kin cells can also be explained by a simulated high-light state of the cells. The CC125_Kin cells were only able to initiate negative phototaxis under light conditions, where the wild-type cells showed positive orientation.

Furthermore, no dark/light adaptive responses were observed in the CC125_Kin cells. Phot is thereby involved in adaptive responses of phototaxis. In a natural environment with a gradual light dispersion, a cell could measure long-term ambient light with altered levels of active Phot. The absorption properties of the LOV domains could thereby serve as an additional blue light avoidance mechanism. In *C. reinhardtii*, K^+ is required for dark adaptation, and it has been shown to be relevant for membrane repolarization after photoexcitation of ChRs (Govorunova et al., 1997). Additionally, cAMP is involved in the regulation of the phototaxis sign. Low cAMP levels cause negative phototaxis, whereas high cAMP levels induce positive phototactic behavior (Boonyareth et al., 2009). The exact mechanisms underlying these cAMP-dependent changes are not yet understood. We know that chlamyrhodopsin-5 possesses a cyclase domain (Kateriya et al., 2004) and has been recently localized in the eyespot by indirect immunofluorescence (Luck et al., 2012); therefore, light signals might be linked to local changes in the cyclic nucleotide levels that are in close proximity to the eyespot. Cyclic nucleotide-gated K^+ channels or other ion channels/pumps important for membrane potential regulation might be among the targets of CrPhot. In *Arabidopsis* guard cell protoplasts, Phot activates a H^+-ATPase, causing a K^+ influx via inward-rectifying K^+-channels and thus regulates stomata opening (Shimazaki et al., 2007; Inoue et al., 2010).

Overexpression of the kinase domain in *C. reinhardtii* also likely affects the plasma membrane potential and ChR-mediated signaling from the eyespot to the flagella. Phot targets that affect the electrical potential of the plasma membrane might also be responsible for the observed effects on dark adaptation. However, CrPhot is also found in the cytoplasm and the axonemes (Huang et al., 2004), so additional targets that affect phototaxis might also be directly localized in the flagella. Phosphorylation events in the axoneme are known to directly affect phototactic behavior (King and Dutcher, 1997).

The unexpected results of our study include the physiological responses observed upon overexpression of the LOV1+LOV2 fragment on eyespot size and phototactic behavior and the similarity to the responses after overexpression of the kinase domain. Our current model to explain these findings is that degradation of full-length CrPhot into smaller PhotΔ20 species is a light-regulated process; therefore, the actual ratio of crPhot to PhotΔ20 reflects the actual light environment. As already discussed, we speculate that the fully active Phot and the PhotΔ20 might act synergistically during signaling. Phots are known to dimerize and cross-phosphorylate, and the kinase alone can bind to LOV2 without a physical linker (Matsuoka and Tokutomi, 2005; Kutta et al., 2008; Nakasako et al., 2008; Kaiserli et al., 2009). We believe that overexpression of the kinase causes cross-phosphorylation of endogenous Phot, followed by degradation of full-length Phot into PhotΔ20 to an extent observed under high light. Overexpressing the LOV1+LOV2 fragment artificially mimics a similar situation. In the PhotΔ20 form, the LOV domains might also interact with either other kinases or proteins that exhibit structural similarities to the Phot kinase domain. Such interactions are possible, both in the light-activated state and in the dark. The effects of overexpression of the inactivated LOV1+LOV2 fragment, which represents the dark state of both LOV domains, and an additional dark incubation on phototactic behavior of such strains supports the above suggestion. This treatment probably caused a saturation of these binding sites because the activated endogenous Phot was unavailable and the inactivated LOV1+LOV2 fragment cannot dissociate from the target site(s) upon illumination. In this model, the time constant of the photocycle and/or the lifetime of the truncated CrPhot may serve as timer(s) for target interaction(s). The dark regeneration rate of CrPhot is more similar to Phot1 of vascular plants, which has a lower light threshold for signaling than Phot2 (Sakai et al., 2001; Kasahara et al., 2002; Guo et al., 2005).

In summary, we have shown that Phot affects the "eye" of this alga in multiple ways. In the long term, Phot affects eyespot size. On an intermediate time scale, Phot adjusts its sensitivity to the ambient light conditions by regulating actual ChR1 levels. More generally, Phot fine-tunes the phototactic response (e.g., sign and adaptation). One major goal for future work will be to identify CrPhot interaction partners. This knowledge is indispensable for deciphering the mechanism of Phot function in this unicellular model alga.

METHODS

Strains and Culture Conditions

Chlamydomonas reinhardtii strain 73.72 mt^+ was obtained from Sammlung für Algenkulturen; strains CC124 mt^-, CC125 mt^+, CC620 mt^+, CC621mt^-, CC806, and CC3403 mt^- were obtained from the *Chlamydomonas* Stock Center (University of Minnesota, St. Paul, MN); strain MS-325 was obtained from M. Schroda (Technical University Kaiserslautern, Germany); and strain CC-4051 was obtained from R.M. Dent (University of California, Berkley, CA). $\Delta Phot^{G5}$ (G5 in Zorin et al., 2009) and its parental strain, 302cw, were from P. Hegemann. The ChR1 knockout strains ZF37-H2 and ZF37-H4 were also generated in the 302cw background by I. Sizova and A. Greiner, and, like strain cw15ArgA, obtained from P. Hegemann. *Tetraselmis astigmatica* was obtained from M. Melkonian (University Cologne, Germany).

T. astigmatica was grown in artificial seawater media (ASPH) supplemented, except where indicated, with 1% Glc and 0.01% yeast extract. Most *C. reinhardtii* strains were grown in standard TAP liquid media. $\Delta Phot^{G5}$, the corresponding parental strain 302cw, and most CrPhot overexpressing strains were grown in TAP media supplemented with 0.05% Arg (Harris, 2009; Zorin et al., 2009) and either in liquid or on agar plates (1.5%). The following mutant strains with inactivated domains (indicated by strikethrough) were cultured in TAP supplemented with 3% tryptone, 2% yeast extract, 0.05% Arg, and 50 μg mL^{-1} ampicillin (TAPTY), either on agar plates or in liquid: $\Delta Phot^{G5}$_Phot_~~L1+L2~~, $\Delta Phot^{G5}$_~~L1~~+L2, and $\Delta Phot^{G5}$_L1+~~L2~~. Strains that overexpressed CrPhot constructs, in the wild-type background of strain MS325, were cultured in TAPTY. Where indicated, cells were additionally grown in minimal medium (Harris, 2009).

Gametes were induced by transfer of cells to nitrogen-free minimal medium (NMM; 3.1 mM K_2HPO_4, 3.4 mM KH_2PO_4, 81 μM $MgSO_4$, and 100 μM $CaCl_2$, pH 7.0) for either 1 or 2 d, under permanent illumination. Cultures were maintained in batch cultures and, unless stated otherwise, were placed in either a 14/10-h light/dark cycle or complete darkness at 15°C ± 1°C for the indicated times. Light-grown cultures were illuminated with either white fluorescent lamps or light-emitting diodes using the indicated wavelengths and light intensities. Standard intensities during growth were 40 to 60 μmol photons m^{-2} s^{-1} of white light. Combinations of different neutral density filters (LOT) were used to obtain low light conditions. The given intensities were equivalent to the mean of intensity values measured before and at the end of each experiment.

Plasmids and Transformation of *C. reinhardtii*

The PsaD promoter and terminator were used for expression of full-length Phot cDNA (amino acids 1 to 750), the LOV domains (L1+L2, amino acids 1 to 363), and the kinase domain (amino acids 358 to 750). All constructs were C-terminal fusions to the Zeocin resistance marker *sh*-Ble. Transformation of cells was performed according to Kindle (1990), using 2 to 5 μg of linearized plasmid DNA per transformation. Strains with cell walls were pretreated with autolysin (Harris, 2009). Selection on TAP-agar plates was performed with 5 to 10 μg mL^{-1} Zeocin. L1+L2 constructs had to be selected in a 12/12-h light/dark cycle, but Phot- and Kin-expressing mutants could be selected under continuous illumination. Expression products were detected by protein immunoblotting (see Supplemental Figure 6 online) using an anti-*sh*-Ble antibody (Cayla). A summary of the constructs used and of the abbreviations of the generated transformants and their characteristics is presented in Supplemental Table 1 online. As is well known for *C. reinhardtii*, many transformants were unstable over a long time period.

Microscopy and Statistical Analyses

Cells that were grown in liquid media were used in eyespot size analyses. *C. reinhardtii* strains were routinely analyzed 4 to 6 d after transfer into fresh medium, whereas *T. astigmatica* was used after 14 to 22 d of growth. Cells for eyespot area determination were analyzed, without fixation, using an Eclipse 800 microscope (Nikon, Plan Apo ×100, 1.4–numerical aperture oil immersion objective) and differential interference contrast microscopy. Eyespot contrast was improved using a green filter. Pictures were captured with a DS-Qi1 cooled charge-coupled device camera that was driven by NIS-Elements BR 3.1 software (Nikon). Only images where both the entire circumference of the eyespot was visible and its surface was fully oriented toward the objective in the focal plane were used for analyses. Cells with "edge-on" and partially visible eyespots were excluded. To avoid biased analyses, we randomly selected cells in the order they were found in the sample. For *C. reinhardtii*, images from 50 to 350 cells were taken for each condition, strain, or clone. For *T. astigmatica*, 35 to 90 cells were analyzed. The eyespot area was manually determined by outlining its circumference with NIS-Elements software (Nikon).

Statistical analyses (two-tailed Student's *t* test, one-way analysis of variance [ANOVA]; Gaussian distribution was always fulfilled) were done using the GraphPad Prism 5 software. Indirect immunofluorescence analyses were conducted using a polyclonal rabbit anti-C-terminal ChR1 serum (1:125) and a monoclonal mouse antiacetylated tubulin (1:600, clone 6-11B; Sigma-Aldrich; Piperno and Fuller, 1985). Cells from log phase cultures were harvested by centrifugation (500*g*, 15 min), resuspended in a small volume of PBS and kept for 5 min on ice. Cells were spotted on three-well, poly-L-Lys–coated slides and then allowed to settle for 10 min at room temperature. Next, slides were dipped into −20°C methanol for 20 to 30 s, briefly dried, and blocked (PBS, 0.1% Tween 20, and 3% BSA; 60 min, 37°C). The cells were incubated overnight, with the primary antibodies in block buffer without Tween at 4°C, washed four times for 5 min each in PBS, and blocked again for 60 min at 37°C. Incubation with both a goat anti-rabbit Alexa 488 secondary antibody and a goat anti-mouse Alexa 594 secondary antibody (Invitrogen; both diluted 1:1000 in block buffer without Tween) was performed for 90 min at 37°C, followed by two 5-min wash steps with PBS and a final mounting in PBS/glycerol (1:1). Fluorescence was viewed with the Eclipse 800 microscope and the equipment described above, using appropriate filter sets. Images were adjusted for brightness and contrast, colored (red for Alexa 488 and green for Alexa 594), and merged using NIS-Elements software.

Protein Extraction and Electrophoretic Methods

Directly prior to cell harvesting, phenylmethylsulfonyl fluoride (1 mM final concentration) was added to the cultures. Log phase cells were harvested, after 4 to 6 d of growth, by centrifugation (2000*g*, 10 min, 4°C), and frozen in liquid nitrogen. Pellets were resuspended in TNED buffer (20 mM Tris, 80 mM NaCl, 1 mM EDTA, and 1 mM DTT, pH 7.5) and supplemented with 1 mM phenylmethylsulfonyl fluoride and a Roche protease inhibitor cocktail, according to the instructions of the supplier. Dark-grown cells were harvested under a dim red safety light, keeping light exposure as short as possible. Then, 300-μL aliquots of the resuspended pellets were either directly mixed with methanol:chloroform (2:1, v:v; 1200 μL) or, in the case of cell wall–possessing strains, homogenized by sonication (four cycles, 15 s each, interrupted by a 15-s cooling phase; 25% output intensity) prior to the addition of methanol/chloroform. Lipid removal, protein precipitation, quantification, and SDS-PAGE (high Tris system) were conducted as described by Schmidt et al. (2006). Loading was based on equal protein content. Immunoblot analyses were performed according to standard techniques. For quantification, at least two internal standards on each blot were used. Primary rabbit antibodies against the *C. reinhardtii* Phot LOV1 domain (Zorin et al., 2009), the *sh*-Ble protein (Cayla-InvivoGen), and either ChR 1 or 2 (S. Kateriya), were used at the indicated dilutions. An anti-rabbit IgG alkaline phosphatase–conjugated antiserum (either 1:2000 or 1:5000) was used for detection. Eyespot fractions were isolated according to Schmidt et al. (2006). Images for figures were processed with Photoshop (Adobe Systems).

Phototaxis Assay

Phototactic orientation was measured in a custom-made, light-scattering apparatus (Schaller et al., 1997). Strain CC806, which only shows negative phototaxis, was used as a reference. Cells were transferred to NMM and incubated in light (>12 h) to induce gametogenesis. In preliminary experiments, we were looking for differences in behavior that depended on the cation composition of the assay media. Experiments using our standard media that contained 10 mM K^+ strains CC125 and CC125_Kin did not reveal significant differences in behavior. By contrast, in the absence of additional K^+, CC125_Kin showed even stronger responses, whereas CC125 signals decreased over time, as expected, since K^+ is needed for membrane repolarization after light excitation (Govorunova et al., 1997). Because of these differences in K^+-dependent responses and for better comparison with previous electrophysiological measurements, gametes were transferred into 10 mM HEPES, 81 μM $MgSO_4$, and 100 μM $CaCl_2$, at pH 6.0, without the addition of potassium. Dark/light adaptation was done by splitting the cultures in two, with one half being placed in a flask covered with aluminum foil and the other half being left in an uncovered flask. Dark adaptation was allowed to continue for at least 1 h. For excitation, LEDs of 405 nm (150 μmol photons m^{-2} s^{-1}) and 470 nm (20 μmol photons m^{-2} s^{-1}) were used.

Accession Numbers

Sequence data of genes encoding the proteins studied in this article can be found in the GenBank/EMBL databases under the following accession numbers: CrPhot, EDP03413.1; ChR1, AAL08946.1; and ChR2, EDP06700.1.

Supplemental Data

The following materials are available in the online version of this article.

Supplemental Figure 1. Protein Blot Analyses of Crude Extracts from ΔChr1 Strains, with an Anti-ChR1 Serum, and Crude Extracts and Eyespot Fractions of $\Delta Phot^{G5}$ and 302cw Cells, with an Anti-LOV1 Serum.

Supplemental Figure 2. Eyespot Area and Cell Size Are Not Correlated in Strains $\Delta Phot^{G5}$, $\Delta Phot^{G5}$_Phot, and $\Delta Phot^{G5}$_Kin.

Supplemental Figure 3. Overexpression of Phot Constructs, in a Background with Wild-Type Levels of Endogenous Phot, Confirm Its Involvement in Eyespot Size Regulation.

Supplemental Figure 4. Overexpression of the Phot Kinase Domain in the Flagellated, Cell Wall–Possessing Strain CC125 Results in Increased Palmelloid Formation.

Supplemental Figure 5. ChR1 Levels in Strains ΔPhot^{G5}_~~L1~~+L2 and ΔPhot^{G5}_L1+~~L2~~ Do Not Decrease.

Supplemental Figure 6. Immunoblot Detection of Expressed Ble:Phot Constructs in Crude Extracts from ΔPhot^{G5} Transformants, Using an anti-*sh*-Ble Serum (1:2000).

Supplemental Table 1. Abbreviations and Descriptions of *C. reinhardtii* Phot Transformants Used in This Study.

ACKNOWLEDGMENTS

We thank Anne Mollwo and Margrit Michalsky for excellent technical assistance and Andre Kraus for help during eyespot isolation. This work was supported by the Universitätsbund Erlangen-Nürnberg e.V. (G.K.) and the German Research Foundation Deutsche Forschungsgemeinschaft (FOR1261, HE-3824/19-1, and 20-1).

AUTHOR CONTRIBUTIONS

G.K., A.G., J.T., and P.H. designed the research. J.T., A.G., M.N., T.R., J.S., Y.L., and G.K. performed the experiments. S.K. contributed the affinity-purified ChR1 and ChR2 antisera. J.T., A.G., M.N., T.R., and G.K. analyzed the data. A.G. and G.K. wrote the article, with contributions and edits from P.H.

Received August 1, 2012; revised October 21, 2012; accepted November 9, 2012; published November 30, 2012.

REFERENCES

Boonyareth, M., Saranak, J., Pinthong, D., Sanvarinda, Y., and Foster, K.W. (2009). Roles of cyclic AMP in regulation of phototaxis in *Chlamydomonas reinhardtii.* Biologia **64:** 1058–1065.

Boyd, J.S., Gray, M.M., Thompson, M.D., Horst, C.J., and Dieckmann, C.L. (2011a). The daughter four-membered microtubule rootlet determines anterior-posterior positioning of the eyespot in *Chlamydomonas reinhardtii*. Cytoskeleton (Hoboken) **68:** 459–469.

Boyd, J.S., Lamb, M.R., and Dieckmann, C.L. (2011b). Miniature- and multiple-eyespot loci in *Chlamydomonas reinhardtii* define new modulators of eyespot photoreception and assembly. G3 (Bethesda) **1:** 489–498.

Boyd, J.S., Mittelmeier, T.M., and Dieckmann, C.L. (2011c). New insights into eyespot placement and assembly in *Chlamydomonas*. BioArchitecture **1:** 196–199.

Boyd, J.S., Mittelmeier, T.M., Lamb, M.R., and Dieckmann, C.L. (2011d). Thioredoxin-family protein EYE2 and Ser/Thr kinase EYE3 play interdependent roles in eyespot assembly. Mol. Biol. Cell **22:** 1421–1429.

Briggs, W.R., et al. (2001). The phototropin family of photoreceptors. Plant Cell **13:** 993–997.

Christie, J.M. (2007). Phototropin blue-light receptors. Annu. Rev. Plant Biol. **58:** 21–45.

Christie, J.M., Salomon, M., Nozue, K., Wada, M., and Briggs, W.R. (1999). LOV (light, oxygen, or voltage) domains of the blue-light photoreceptor phototropin (nph1): Binding sites for the chromophore flavin mononucleotide. Proc. Natl. Acad. Sci. USA **96:** 8779–8783.

Christie, J.M., Swartz, T.E., Bogomolni, R.A., and Briggs, W.R. (2002). Phototropin LOV domains exhibit distinct roles in regulating photoreceptor function. Plant J. **32:** 205–219.

Crosson, S., and Moffat, K. (2002). Photoexcited structure of a plant photoreceptor domain reveals a light-driven molecular switch. Plant Cell **14:** 1067–1075.

de Carbonnel, M., Davis, P., Roelfsema, M.R., Inoue, S., Schepens, I., Lariguet, P., Geisler, M., Shimazaki, K., Hangarter, R., and Fankhauser, C. (2010). The *Arabidopsis* PHYTOCHROME KINASE SUBSTRATE2 protein is a phototropin signaling element that regulates leaf flattening and leaf positioning. Plant Physiol. **152:** 1391–1405.

Demarsy, E., and Fankhauser, C. (2009). Higher plants use LOV to perceive blue light. Curr. Opin. Plant Biol. **12:** 69–74.

Ermilova, E.V., Zalutskaya, Z.M., Huang, K.Y., and Beck, C.F. (2004). Phototropin plays a crucial role in controlling changes in chemotaxis during the initial phase of the sexual life cycle in *Chlamydomonas*. Planta **219:** 420–427.

Fedorov, R., Schlichting, I., Hartmann, E., Domratcheva, T., Fuhrmann, M., and Hegemann, P. (2003). Crystal structures and molecular mechanism of a light-induced signaling switch: The Phot-LOV1 domain from *Chlamydomonas reinhardtii*. Biophys. J. **84:** 2474–2482.

Folta, K.M., and Kaufman, L.S. (2003). Phototropin 1 is required for high-fluence blue-light-mediated mRNA destabilization. Plant Mol. Biol. **51:** 609–618.

Foster, K.W., and Smyth, R.D. (1980). Light antennas in phototactic algae. Microbiol. Rev. **44:** 572–630.

Fuhrmann, M., Hausherr, A., Ferbitz, L., Schödl, T., Heitzer, M., and Hegemann, P. (2004). Monitoring dynamic expression of nuclear genes in *Chlamydomonas reinhardtii* by using a synthetic luciferase reporter gene. Plant Mol. Biol. **55:** 869–881.

Govorunova, E.G., Jung, K.-H., Sineshchekov, O.A., and Spudich, J.L. (2004). *Chlamydomonas* sensory rhodopsins A and B: cellular content and role in photophobic responses. Biophys. J. **86:** 2342–2349.

Govorunova, E.G., Sineshchekov, O.A., and Hegemann, P. (1997). Desensitization and dark recovery of the photoreceptor current in *Chlamydomonas reinhardtii*. Plant Physiol. **115:** 633–642.

Guo, H., Kottke, T., Hegemann, P., and Dick, B. (2005). The phot LOV2 domain and its interaction with LOV1. Biophys. J. **89:** 402–412.

Harper, S.M., Neil, L.C., and Gardner, K.H. (2003). Structural basis of a phototropin light switch. Science **301:** 1541–1544.

Harris, E.H. (2009). The *Chlamydomonas* Sourcebook, 2nd ed, Vol. 1. (New York: Elsevier).

Harz, H., Nonnengässer, C., and Hegemann, P. (1992). The photoreceptor current of the green alga *Chlamydomonas*. Philos. Trans. R. Soc. Lond. B Biol. Sci. **338:** 39–52.

Hegemann, P., and Berthold, P. (2009). Sensory photoreceptors and light control of flagellar activity. In The *Chlamydomonas* Sourcebook, 2nd ed, Vol. 3, G.B. Witman, ed (San Diego: Academic Press) pp. 395–429.

Holmes, J.A., and Dutcher, S.K. (1989). Cellular asymmetry in *Chlamydomonas reinhardtii*. J. Cell Sci. **94:** 273–285.

Huala, E., Oeller, P.W., Liscum, E., Han, I.-S., Larsen, E., and Briggs, W.R. (1997). *Arabidopsis* NPH1: A protein kinase with a putative redox-sensing domain. Science **278:** 2120–2123.

Huang, K., Merkle, T., and Beck, C.F. (2002). Isolation and characterization of a *Chlamydomonas* gene that encodes a putative blue-light photoreceptor of the phototropin family. Physiol. Plant. **115:** 613–622.

Huang, K.Y., and Beck, C.F. (2003). Phototropin is the blue-light receptor that controls multiple steps in the sexual life cycle of the green alga *Chlamydomonas reinhardtii*. Proc. Natl. Acad. Sci. USA **100:** 6269–6274.

Huang, K.Y., Kunkel, T., and Beck, C.F. (2004). Localization of the blue-light receptor phototropin to the flagella of the green alga *Chlamydomonas reinhardtii*. Mol. Biol. Cell **15:** 3605–3614.

Im, C.S., Eberhard, S., Huang, K.Y., Beck, C.F., and Grossman, A.R. (2006). Phototropin involvement in the expression of genes encoding chlorophyll and carotenoid biosynthesis enzymes and LHC apoproteins in *Chlamydomonas reinhardtii*. Plant J. **48:** 1–16.

Inoue, S., Takemiya, A., and Shimazaki, K. (2010). Phototropin signaling and stomatal opening as a model case. Curr. Opin. Plant Biol. **13:** 587–593.

Inoue, S.-I., Kinoshita, T., Matsumoto, M., Nakayama, K.I., Doi, M., and Shimazaki, K.-I. (2008). Blue light-induced autophosphorylation of phototropin is a primary step for signaling. Proc. Natl. Acad. Sci. USA **105:** 5626–5631.

Kagawa, T., and Wada, M. (2002). Blue light-induced chloroplast relocation. Plant Cell Physiol. **43:** 367–371.

Kaiserli, E., Sullivan, S., Jones, M.A., Feeney, K.A., and Christie, J.M. (2009). Domain swapping to assess the mechanistic basis of *Arabidopsis* phototropin 1 receptor kinase activation and endocytosis by blue light. Plant Cell **21:** 3226–3244.

Kasahara, M., et al. (2002). Photochemical properties of the flavin mononucleotide-binding domains of the phototropins from *Arabidopsis*, rice, and *Chlamydomonas reinhardtii*. Plant Physiol. **129:** 762–773.

Kateriya, S., Nagel, G., Bamberg, E., and Hegemann, P. (2004). "Vision" in single-celled algae. News Physiol. Sci. **19:** 133–137.

Kindle, K.L. (1990). High-frequency nuclear transformation of *Chlamydomonas reinhardtii*. Proc. Natl. Acad. Sci. USA **87:** 1228–1232.

King, S.J., and Dutcher, S.K. (1997). Phosphoregulation of an inner dynein arm complex in *Chlamydomonas reinhardtii* is altered in phototactic mutant strains. J. Cell Biol. **136:** 177–191.

Kinoshita, T., Doi, M., Suetsugu, N., Kagawa, T., Wada, M., and Shimazaki, K. (2001). Phot1 and phot2 mediate blue light regulation of stomatal opening. Nature **414:** 656–660.

Kinoshita, T., Emi, T., Tominaga, M., Sakamoto, K., Shigenaga, A., Doi, M., and Shimazaki, K.-I. (2003). Blue-light- and phosphorylation-dependent binding of a 14-3-3 protein to phototropins in stomatal guard cells of broad bean. Plant Physiol. **133:** 1453–1463.

Kong, S.-G., Kinoshita, T., Shimazaki, K.-I., Mochizuki, N., Suzuki, T., and Nagatani, A. (2007). The C-terminal kinase fragment of *Arabidopsis* phototropin 2 triggers constitutive phototropin responses. Plant J. **51:** 862–873.

Kong, S.G., Suzuki, T., Tamura, K., Mochizuki, N., Hara-Nishimura, I., and Nagatani, A. (2006). Blue light-induced association of phototropin 2 with the Golgi apparatus. Plant J. **45:** 994–1005.

Kreimer, G. (1994). Cell biology of phototaxis in flagellated algae. Int. Rev. Cytol. **148:** 229–310.

Kreimer, G. (2001). Light reception and signal modulation during photoorientation of flagellate algae. In Comprehensive Series in Photosciences, M. Lebert and D.-P. Häder, eds (Amsterdam: Elsevier/North Holland), pp. 193–227.

Kreimer, G. (2009). The green algal eyespot apparatus: A primordial visual system and more? Curr. Genet. **55:** 19–43.

Kreimer, G., and Melkonian, M. (1990). Reflection confocal laser scanning microscopy of eyespots in flagellated green algae. Eur. J. Cell Biol. **53:** 101–111.

Kreimer, G., Overländer, C., Sineshchekov, O.A., Stolzis, H., Nultsch, W., and Melkonian, M. (1992). Functional analysis of the eyespot in *Chlamydomonas reinhardtii* mutant ey 627, mt. Planta **188:** 513–521.

Kutta, R.J., Hofinger, E.S.A., Preuss, H., Bernhardt, G., and Dick, B. (2008). Blue-light induced interaction of LOV domains from *Chlamydomonas reinhardtii*. ChemBioChem **9:** 1931–1938.

Liscum, E., and Briggs, W.R. (1995). Mutations in the NPH1 locus of *Arabidopsis* disrupt the perception of phototropic stimuli. Plant Cell **7:** 473–485.

Luck, M., Mathes, T., Bruun, S., Fudim, R., Hagedorn, R., Nguyen, T.M. T., Kateriya, S., Kennis, J.T.M., Hildebrandt, P., and Hegemann, P. (2012). A photochromic histidine kinase rhodopsin (HKR1) that is bimodally switched by UV and blue light. J. Biol. Chem. **287:** 40083–40090.

Matsuoka, D., and Tokutomi, S. (2005). Blue light-regulated molecular switch of Ser/Thr kinase in phototropin. Proc. Natl. Acad. Sci. USA **102:** 13337–13342.

Mittag, M., Kiaulehn, S., and Johnson, C.H. (2005). The circadian clock in *Chlamydomonas reinhardtii*. What is it for? What is it similar to? Plant Physiol. **137:** 399–409.

Mittelmeier, T.M., Berthold, P., Danon, A., Lamb, M.R., Levitan, A., Rice, M.E., and Dieckmann, C.L. (2008). C2 domain protein MIN1 promotes eyespot organization in *Chlamydomonas reinhardtii*. Eukaryot. Cell **7:** 2100–2112.

Mittelmeier, T.M., Boyd, J.S., Lamb, M.R., and Dieckmann, C.L. (2011). Asymmetric properties of the *Chlamydomonas reinhardtii* cytoskeleton direct rhodopsin photoreceptor localization. J. Cell Biol. **193:** 741–753.

Nagel, G., Ollig, D., Fuhrmann, M., Kateriya, S., Musti, A.M., Bamberg, E., and Hegemann, P. (2002). Channelrhodopsin-1: A light-gated proton channel in green algae. Science **296:** 2395–2398.

Nagel, G., Szellas, T., Huhn, W., Kateriya, S., Adeishvili, N., Berthold, P., Ollig, D., Hegemann, P., and Bamberg, E. (2003). Channelrhodopsin-2, a directly light-gated cation-selective membrane channel. Proc. Natl. Acad. Sci. USA **100:** 13940–13945.

Nakasako, M., Zikihara, K., Matsuoka, D., Katsura, H., and Tokutomi, S. (2008). Structural basis of the LOV1 dimerization of *Arabidopsis* phototropins 1 and 2. J. Mol. Biol. **381:** 718–733.

Ohgishi, M., Saji, K., Okada, K., and Sakai, T. (2004). Functional analysis of each blue light receptor, cry1, cry2, phot1, and phot2, by using combinatorial multiple mutants in *Arabidopsis*. Proc. Natl. Acad. Sci. USA **101:** 2223–2228.

Onodera, A., Kong, S.G., Doi, M., Shimazaki, K., Christie, J., Mochizuki, N., and Nagatani, A. (2005). Phototropin from *Chlamydomonas reinhardtii* is functional in *Arabidopsis thaliana*. Plant Cell Physiol. **46:** 367–374.

Pazour, G.J., Agrin, N., Leszyk, J., and Witman, G.B. (2005). Proteomic analysis of a eukaryotic cilium. J. Cell Biol. **170:** 103–113.

Pfeifer, A., Mathes, T., Lu, Y., Hegemann, P., and Kottke, T. (2010). Blue light induces global and localized conformational changes in the kinase domain of full-length phototropin. Biochemistry **49:** 1024–1032.

Piperno, G., and Fuller, M.T. (1985). Monoclonal antibodies specific for an acetylated form of α-tubulin recognize the antigen in cilia and flagella from a variety of organisms. J. Cell Biol. **101:** 2085–2094.

Prochnik, S.E., et al. (2010). Genomic analysis of organismal complexity in the multicellular green alga *Volvox carteri*. Science **329:** 223–226.

Reisdorph, N.A., and Small, G.D. (2004). The CPH1 gene of *Chlamydomonas reinhardtii* encodes two forms of cryptochrome whose levels are controlled by light-induced proteolysis. Plant Physiol. **134:** 1546–1554.

Roberts, D.G.W., Lamb, M.R., and Dieckmann, C.L. (2001). Characterization of the *EYE2* gene required for eyespot assembly in *Chlamydomonas reinhardtii*. Genetics **158:** 1037–1049.

Sakamoto, K., and Briggs, W.R. (2002). Cellular and subcellular localization of phototropin 1. Plant Cell **14:** 1723–1735.

Sakai, T., Kagawa, T., Kasahara, M., Swartz, T.E., Christie, J.M., Briggs, W.R., Wada, M., and Okada, K. (2001). *Arabidopsis* nph1 and npl1: blue light receptors that mediate both phototropism and chloroplast relocation. Proc. Natl. Acad. Sci. USA **98:** 6969–6974.

Salomon, M., Knieb, E., von Zeppelin, T., and Rüdiger, W. (2003). Mapping of low- and high-fluence autophosphorylation sites in phototropin 1. Biochemistry **42:** 4217–4225.

Schaller, K., David, R., and Uhl, R. (1997). How *Chlamydomonas* keeps track of the light once it has reached the right phototactic orientation. Biophys. J. **73:** 1562–1572.

Schmidt, M., et al. (2006). Proteomic analysis of the eyespot of *Chlamydomonas reinhardtii* provides novel insights into its components and tactic movements. Plant Cell **18:** 1908–1930.

Shimazaki, K.-I., Doi, M., Assmann, S.M., and Kinoshita, T. (2007). Light regulation of stomatal movement. Annu. Rev. Plant Biol. **58:** 219–247.

Sineshchekov, O.A., Govorunova, E.G., and Spudich, J.L. (2009). Photosensory functions of channelrhodopsins in native algal cells. Photochem. Photobiol. **85:** 556–563.

Sineshchekov, O.A., Jung, K.-H., and Spudich, J.L. (2002). Two rhodopsins mediate phototaxis to low- and high-intensity light in *Chlamydomonas reinhardtii*. Proc. Natl. Acad. Sci. USA **99:** 8689–8694.

Sullivan, S., Thomson, C.E., Kaiserli, E., and Christie, J.M. (2009). Interaction specificity of *Arabidopsis* 14-3-3 proteins with phototropin receptor kinases. FEBS Lett. **583:** 2187–2193.

Sullivan, S., Thomson, C.E., Lamont, D.J., Jones, M.A., and Christie, J.M. (2008). In vivo phosphorylation site mapping and functional characterization of *Arabidopsis* phototropin 1. Mol. Plant **1:** 178–194.

Takemiya, A., Inoue, S., Doi, M., Kinoshita, T., and Shimazaki, K. (2005). Phototropins promote plant growth in response to blue light in low light environments. Plant Cell **17:** 1120–1127.

Tokutomi, S., Matsuoka, D., and Zikihara, K. (2008). Molecular structure and regulation of phototropin kinase by blue light. Biochim. Biophys. Acta **1784:** 133–142.

Tseng, T.-S., and Briggs, W.R. (2010). The *Arabidopsis* rcn1-1 mutation impairs dephosphorylation of Phot2, resulting in enhanced blue light responses. Plant Cell **22:** 392–402.

Wagner, V., Ullmann, K., Mollwo, A., Kaminski, M., Mittag, M., and Kreimer, G. (2008). The phosphoproteome of a *Chlamydomonas reinhardtii* eyespot fraction includes key proteins of the light signaling pathway. Plant Physiol. **146:** 772–788.

Zorin, B., Lu, Y., Sizova, I., and Hegemann, P. (2009). Nuclear gene targeting in Chlamydomonas as exemplified by disruption of the PHOT gene. Gene **432:** 91–96.

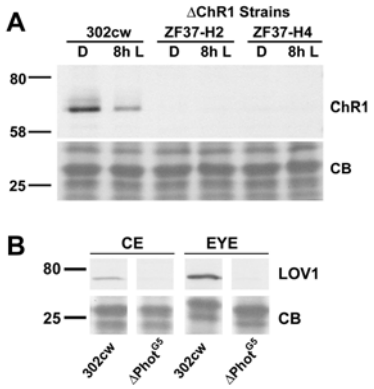

Supplemental Figure 1. Protein Blot Analyses of Crude Extracts from ΔChr1 Strains, with an anti-ChR1 Serum, and Crude Extracts and Eyespot Fractions of ΔPhot^{G5} and 302cw Cells, with an anti-LOV1 Serum. **(A)** Crude extracts (8 µg) of the two ΔChr1 strains (ZF37-H; ZF37-H4) and the parental strain 302cw were separated by SDS-PAGE (11%) and probed with an anti-ChR1 serum (ChR1, 1:5000). Equal protein loading was verified by Coomassie Blue (CB) staining of the lower part of the blot. **(B)** Eight micrograms of crude extracts (CE) or isolated eyespots (EYE) of ΔPhot^{G5} and its parental strain 302cw was separated by SDS-PAGE, blotted and probed with an anti-LOV1 serum (LOV1, 1:2000). Equal loading was verified by CB staining of the lower part of the blot. Developing times were identical for each lane.

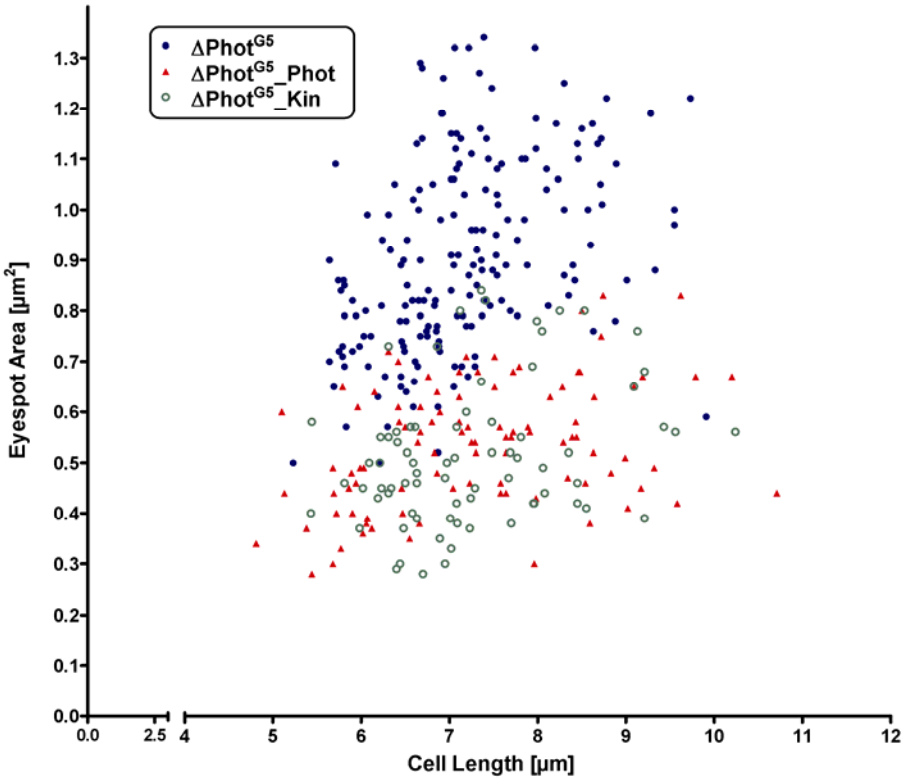

Supplemental Figure 2. Eyespot Area and Cell Size are not Correlated in Strains ΔPhot^{G5}, ΔPhot^{G5}_Phot, and ΔPhot^{G5}_Kin. Eyespot area was determined as described (see Methods) and the longest cell axis was used to determine the cell length of the same cell.

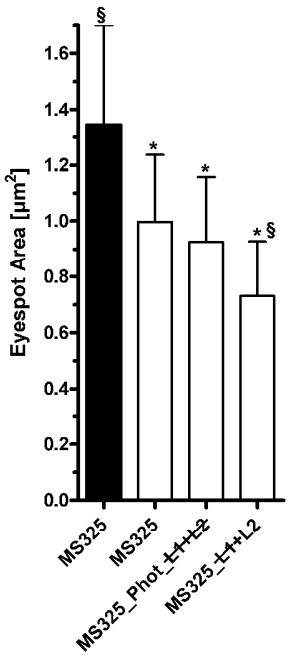

Supplemental Figure 3. Over-Expression of Phot Constructs, in a Background with Wild-type Levels of Endogenous Phot, Confirm its Involvement in Eyespot Size Regulation. MS325 (wild-type strain), MS325_Phot_~~L1+L2~~ (strain expressing full-length Phot with both LOV domains inactivated by point mutation: C57S and C250S), MS325_~~L1~~+L2 (strain expressing the N-terminal part of Phot with an inactivated LOV1 domain). Black columns: dark-grown cells; white columns: cells were grown in a 14/10 h light/dark cycle. Data are mean ± S.D.; n = 101 – 109 cells; * indicate values that were determined by Student´s t test to be significantly different from the eyespot size of dark grown cells and § for comparison to the MS325 cells grown under a light/dark cycle ($p < 0.0001$).

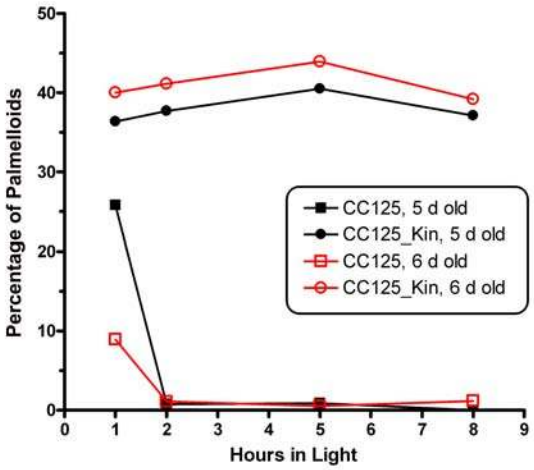

Supplemental Figure 4. Over-Expression of the Phot Kinase Domain in the Flagellated, Cell-Wall Possessing Strain CC125 Results in Increased Palmelloid Formation.
For determination of palmelloids, 200 µl cells from 5- or 6-day-old cultures was fixed with 200 µl 1% iodine-potassium-iodide solution and analyzed under phase contrast microscopy. For each data point about 200 cells were scored.

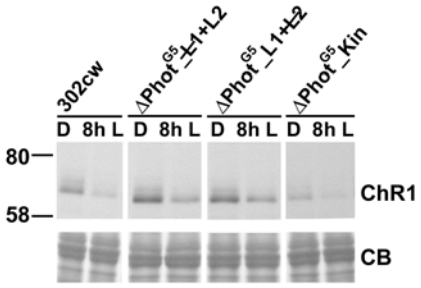

Supplemental Figure 5. ChR1 Levels in Strains ΔPhot^{G5}_~~L1~~+L2 and ΔPhot^{G5}_L1+~~L2~~ do not Decrease. Crude extracts were made either directly before (D) or 8 h after the onset of illumination (8h L). Equal protein loading was verified by Coomassie Blue (CB) staining. Blots were equally developed. For further experimental details see Methods.

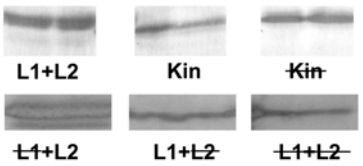

Supplemental Figure 6. Immunoblot Detection of Expressed Ble:Phot Constructs in Crude Extracts from ΔPhot^{G5} Transformants, using an anti-*sh*-Ble Serum (1:2000). ~~Kin =~~ point-mutation inactivated Kin (D547N); ~~L1~~+L2 = N-terminal domain with inactivated LOV1 (C57S); L1+~~L2 =~~ N-terminal domain with inactivated LOV2 (C250S); ~~L1+L2~~ = construct with both LOV domains inactivated (C57S and C250S).

Supplemental Table 1. Abbreviations and descriptions of *C. reinhardtii* Phot transformants used in this study.

Transformant strain	Phototropin construct[a,b]	Functional consequences
ΔPhot^{G5}_Phot	full-length Phot	functional Phot
ΔPhot ^{G5}_Phot_~~L1+L2~~ MS325_Phot_~~L1+L2~~	full-length Phot with point mutated LOV1and LOV2 (C57S and C250S)	permanently inactive Phot
ΔPhot ^{G5}_Kin CC125_Kin	C-terminal kinase fragment	active kinase without light/dark control
ΔPhot ^{G5}_~~Kin~~	point-mutated C-terminal kinase fragment, point mutations either D547N or S611A	inactive kinase disruption of Mg^{2+}-ATP coordination (D547N) or autophosphorylation (S611A)
ΔPhot ^{G5}_L1+L2 CC3403_L1+L2	N-terminal fragment with LOV1and LOV2 domain	functional, light-responsive N-terminus
ΔPhot ^{G5}_~~L1+L2~~ CC3403_~~L1+L2~~	N-terminal fragment with point-mutated LOV1 and LOV2 (C57S and C250S)	disruption of light-activation of both LOV domains
ΔPhot ^{G5}_ L1+~~L2~~	N-terminal fragment with functional LOV1 and point-mutated LOV2 (C250S) domain	disruption of light-activation of LOV2
ΔPhot ^{G5}_~~L1~~+L2 MS325_~~L1~~+L2	N-terminal fragment with point-mutated LOV1 (C57S) and functional LOV2 domain	disruption of light-activation of LOV1

[a] All constructs are N-terminally fused to the Zeocin resistance protein Ble.
[b] All kinase & LOV domain constructs also possess parts of the Jα domain.

Phototropin Influence on Eyespot Development and Regulation of Phototactic Behavior in *Chlamydomonas reinhardtii*

Jessica Trippens, Andre Greiner, Jana Schellwat, Martin Neukam, Theresa Rottmann, Yinghong Lu, Suneel Kateriya, Peter Hegemann and Georg Kreimer

Plant Cell; originally published online November 30, 2012;
DOI 10.1105/tpc.112.103523